Theoretical, Experimental Investigations and Computational Molecular Modeling of Amoxicillin Metal Complexes

Aml Z. Elabdeen[a*], Waheed M. Salem[b], Mohsen M. T. El-Tahawy[c], Alaa E. Ali[c]

[a]Damanhur Joint Lab, Ministry of Health, Egypt
[b]Chemistry Department, Faculty of Applied health sciences technology, Menofia University, Egypt
[c]Chemistry Department, Faculty of science, Damanhur University, Egypt
email:Amlzainelabdeen.emara@gmail.com, Mobile: +201060059510

Abstract Synthesis, physicochemical and thermal characterization of Amoxicillin with transition metals (Fe(III), Mn(II), Ni(II), Cu(II), Zn(II) and Cd(II) were discussed in this study. It's obtained that Amoxicillin act as bidentate ligand. From magnetic measurements and spectral data, octahedral structures were proposed for all complexes except for (Ni) complex which had tetrahedral structure. The biological activity of Amoxicillin complexes showed higher activity than Amoxicillin for some strains. From TG and DTA curves, the thermal decomposition mechanisms of Amoxicillin and its metal complexes were suggested and all kinetic parameters were calculated.
Since previous work had not systematically studied Molecular modeling of the complexes, In this computational study, Molecular Modeling and optimization of Amoxicillin metal complexes were done and all optimized parameters were calculated by Gaussian 09W program using semi empirical and density functional theory basis sets. HOMO-LUMO energy gaps were calculated and also charge transfer between metal atoms and ligand was studied.

Keywords Amoxicillin- Thermal analysis- Molecular Modeling- Optimization – Density functional theory

Introduction

Chemistry of metal-drug compounds and design of more biologically drugs is very important nowadays [1]. Interface of metal ions with any donor ligand provides organically effective compounds of different chemical structures [2]. The study of metal complexes with drugs as ligands is very exciting because of enhancement of the metal action to the activity of the drug [3]. Amoxicillin is one of the important derivatives of semisynthetic penicillins (aminopencillins). It is off white or almost white crystalline powder which is slightly soluble in water and alcohol such as ethanol and methanol [4, 5]. Several research findings in medical science put amoxicillin as an abortive drug that always requires modifications, either by changing the ligand properties or by complexation with some metal ions[6]. The chemical structure of Amoxicillin is illustrated in Fig. 1:
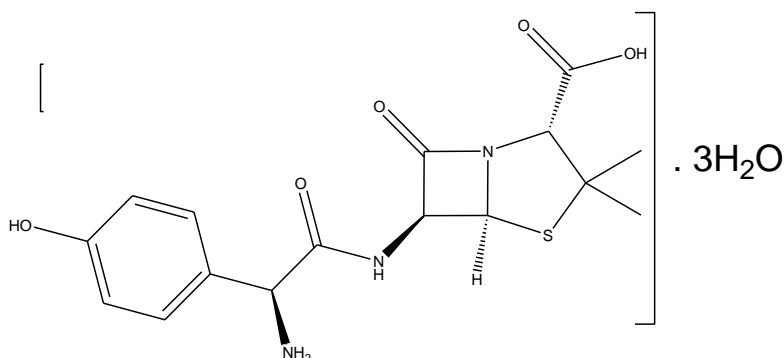
Chemistry Research Journal

Figure 1: Structure of Hydrated Amoxicillin, HL

Many attempts were made to generate new synthesized metal complexes of Amoxicillin. Previous work studied only the synthesis and spectra of complexes [7-9]. In the present work, conformational changes and coordination chemistry of Amoxicillin towards transition metals were identified by IR, electronic spectra, magnetic susceptibility and Electron Spin Resonance (ESR). Biological activity of Amoxicillin and its metal complexes were compared. Also thermal analysis of Amoxicillin and its metal complexes were discussed from thermo-gravimetric and differential thermal analysis curves. Mechanism of decomposition and thermal stability of complexes were discussed in details. Most of the Kinetic parameters were calculated from thermal data. Molecular modeling of complexes was done and all the parameters as bond length, angles were evaluated after optimization of complexes with the lowest energy structures using Gaussview 06 and Gauassian 09W computer programs. HOMO and LUMO structures were determined and energy gaps evaluation was done. All these calculations were done using density functional theory (DFT) which considered as a popular post-Hartree–Fock (HF) approach for the computation of molecular structures, and the energies of molecules. It is extremely useful in the study of the electronic structures of molecules [10].

Experimental

Solutions of ligand and metal salts were prepared with equal molar ratios (1×10^{-3} mol/L). Aqueous solutions of Amoxicillin trihydrate (4.19 g, 10 mmol) was prepared. The pH of solutions was adjusted slightly basic pH (7-8) by adding 2 drops of ammonia solution. The solution was heated till a clear solution was obtained. Aqueous ethanolic (20ml) solutions (1:1) of the metal salts [10mmol, 2.01 g of $CdCl_2.H_2O$], [10 mmol, 1.36 g of $ZnCl_2$], [10mmol, 2.703 g of $FeCl_3.6H_2O$], [10mmol, 2.38 g of $NiCl_2.6H_2O$)], [10mmol, 1.705 g of $CuCl_2.2H_2O$], [10mmol, 1.98 g of $MnCl_2.4H_2O$] were prepared first. A general method has been used for the preparation of the new complexes by the reaction of the metal salts with ligand at a metal to ligand molar ratio of 1:1 [11] and also, The method described by Ogunniran was modified here for the synthesis of all the complexes [12]. The metal salts were added drop by drop to a solution of ligand. The reaction mixture was allowed to stir magnetically for 1 h at room temperature untill the volume of the solution was concentrated to half of the initial volume and then left over-night, where the precipitated complexes were separated by filtration, then washed several times with a mixture of $EtOH-H_2O$ and dried in a vacuum desiccator over anhydrous $CaCl_2$.

Measurements

Carbon, hydrogen, sulphur and nitrogen contents of all the synthesized complexes were recorded on CHNS Nr.11042023 located at central lab, Cairo University. The analysis of chloride content of the complexes was determined by applying the familiar Volhard method [13]. Melting points of the ligand and all prepared complexes were determined on MEL-TEMP II melting point apparatus in open glass capillaries which located in the faculty of science, Damanhour University. The infrared spectra of the ligand and its metal complexes were done using Bruker Tensor 37 FT-IR covering frequency range of 200-4000 cm^{-1}. The spectrophotometric measurements in the Ultraviolet and visible spectra were recorded for solutions using a double beam spectrophotometer US LAB, covering the wavelength range 190-1100 nm. The electronic spectral data of ligands were carried out in DMSO (10^{-}

3Molar) solution [14, 15]. The metal contents were determined based on atomic absorption technique using (PerkinElmer (PinAAcle 900 T)) atomic absorption spectrophotometer. The instrument located at Damanhour Joint lab, Ministry of Health. Molar magnetic susceptibilities, corrected for diamagnetism using Pascal's constants were determined at room temperature (298 °K) using Faraday's method. The instrument was calibrated with Hg [Co(SCN)₄]. Electron spin resonance spectrum was recorded with a reflection spectrometer operating at (9.1-9.8) GegaHertZ in a cylindrical resonance cavity with 100 KiloHertZ modulation. Differential thermal analysis (DTA) and thermogravimetric analysis (TGA) of Amoxicillin and its metal complexes were carried out using a LINSEIS STA PT1000 (TG - DTA/DSC). The instrument located at Central Laboratory, Faculty of Science, Alexandria University. The antimicrobacterial activities of the complexes were tested against some kinds of bacteria comparable with the ampicillin and amoxicillin free drugs. The biological screening and antimicrobial activities of the free ligand and its metal complexes were examined by using well-cut diffusion technique. This was done at Central Laboratory, Faculty of Pharmacy, Alexandria University. They are examined against 5 microorganisms representing different microbial categories, two Gram-positive (Staphylococcus Aureas ATCC6538P and Bacillus subtilis ATCC19659), two Gram negative (Escherischia coli ATCC8739 strain and Pseudomonas aeruginosa ATCC9027) and candida albicans (ATCC2091) as a fungi. Molecular modeling of Amoxicillin and its metal complexes were done by GaussView06 program. Calculations of the optimized parameters (bond length, bond angles and dihedral angles) were done by Gaussian 09W computer program. The optimized conformations with the lowest energy of the individual molecules were determined using dynamic simulations followed by energy minimization to give deep spotlights on the bonding properties and structures of these compounds. Two methods were used in optimization process, Semi empirical (PM6) with basis set (3-21G) and DFT (B3LYP) with basis set (LanL 2DZ).

Results and Discussion

Physical measurements, analytical and spectral data of the Amoxicillin complexes are given in Table 1.

Table 1: Elemental analysis, molecular formula, Molecular weight, Stoichiometries and color of (Amoxicillin) complexes

Complexes	Molecular Formula	Color	Melting point	Calculated / (Found)%						
				C	H	N	S	O	M	Cl
Amoxicillin	$C_{16}H_{19}N_3O_5S$ (365.5)	Off-white	195	45.8 (52.59)	5.96 (5.24)	10.0 (11.5)	7.6 (8.77)	30.64 (21.89)	- -	- -
[Ni(L₂)].H₂O (1:2)	$C_{32}H_{38}N_6NiO_{11}S_2$ (805.5)	yellow	>300	47.69 (47.72)	4.82 (4.76)	10.42 (10.43)	7.91 (7.95)	22.03 (21.85)	7.13 (7.29)	- -
[Fe (L₂) (H₂O) Cl] (1:2)	$C_{32}H_{38}N_6FeO_{11}S_2Cl$ (838)	dark brown	>300	46.01 (45.86)	4.55 (4.57)	9.75 (10.03)	7.99 (7.65)	20.9 (21.0)	6.5 (6.66)	4.3 (4.23)
[Cu (HL₂)(H₂O) Cl] (1:2)	$C_{32}H_{39}N_6CuO_{11}S_2Cl$ (846.5)	green	200	45.14 (45.39)	4.5 (4.64)	9.97 (9.92)	7.63 (7.58)	20.82 (20.78)	7.44 (7.5)	4.5 (4.19)
[Zn (HL)₂ (Cl)₂] (1:2)	$C_{32}H_{38}N_6ZnO_{10}S_2Cl_2$ (867)	yellow	>300	43.95 (44.33)	4.15 (4.42)	9.7 9.69	7.44 (7.39)	19.36 (18.45)	7.6 (7.54)	7.8 (8.18)
[Cd (HL₂) (H₂O) Cl] (1:2)	$C_{32}H_{39}N_6CdO_{11}S_2Cl$ (895.5)	yellow	>300	42.90 (42.91)	4.31 (4.39)	9.17 (9.38)	7.3 (7.16)	20.5 (19.65)	12.32 (12.55)	3.5 (3.96)
[Mn (HL₂) (H₂O) Cl] (1:2)	$C_{32}H_{39}N_6MnO_{11}S_2Cl$ (838)	buff	>300	46.00 (45.85)	4.77 (4.69)	9.77 (10.03)	8.22 (7.65)	20.54 (21.00)	6.5 (6.55)	4.2 (4.23)

FT-IR spectra of Amoxicillin (HL) and its metal complexes

The (FT-IR) spectrum for the ligand (HL), display broad band around 3266 cm^{-1} ascribed to υ (N–H) stretching vibration. The band at 1441 cm^{-1} represents the grouping υ (C–N) cm^{-1} stretching vibration while the band at 1687 cm^{-1} is ascribed to υ (C=O) of Carboxyl group [16]. The band at 1125 cm^{-1} is appointed to υ (C–O) stretching vibration. The bands at 1579 and 1376 cm^{-1} are appointed to stretching absorption carboxylate υ (COO$^-$) group asymmetric and symmetric stretching vibration, respectively. Δυ (COO$^-$) asym - υ (COO$^-$) sym =203 cm^{-1} [17]. The band at 714 cm^{-1} is appointed to υ (C–S) stretching vibration [16]. For Amoxicillin complexes, IR spectra shows a band of N-H stretching vibration of the hydrogen bonded NH$_2$ group which appears at 3266 cm^{-1} in spectra of Amoxicillin (Table 2). This band appears in all simple complexes but overlapped with $ν_{O-H}$ of H$_2$O broad bands. Generally, The carboxyl (C=O) band appears at 1687 cm^{-1} in the spectrum of Amoxicillin is shifted in the simple complexes spectra to (1600 -1650) cm^{-1} range. The band at 1579 cm^{-1}, corresponding to the carboxylate asymmetrical stretching of the free ligand is shifted to lower wave numbers in the spectra of the complexes and this is an indication of coordination through that group [18].

The IR spectra of the complexes give a separation value of > 200 cm^{-1} suggesting monodentate carboxylate. The bonding of oxygen is provided by the presence of bands at (469- 472) cm^{-1} represent (M-O) [19].

Table 2: Relevant infrared frequencies (cm^{-1}) of the Amoxicillin and its metal complexes

Compound	ν N-H	ν NH2	ν(C=O) lactam	ν(C=O) COOH	ν (COO) asym	ν (C-N) of β-lactam	ν (COO) sym	ν C-O stretch	C-H bending	ν C-S stretch	ν M-O stretch
Amoxicillin (HL)	3266	2934	1774	1687	1579	1441	1376	1125	856	714	-
[Fe (L$_2$) (H$_2$O) Cl]	3299	2950	-	1600	1512	1418	1386	1114	840	693	469
[Ni (L$_2$)].H$_2$O	3280	2969	-	1600	1514	1450	1384	1109	837	708	472
[Cu (HL$_2$)(H$_2$O) Cl]	3347	2970	-	1619	1512	1448	1397	1100	840	705	469
[Zn (HL$_2$)$_2$ (Cl)$_2$]	3259	2970	-	1600	1511	1448	1401	1116	837	710	471
[Cd (HL$_2$) (H$_2$O) Cl]	3250	2928	-	1650	1512	1445	1395	1110	835	705	470
[Mn (HL$_2$) (H$_2$O) Cl]	3365	2930	-	1640	1514	1445	1404	1103	860	713	469

Electronic spectral and magnetic studies

The brown electronic absorption spectra of iron-complex [Fe (L$_2$) (H$_2$O) Cl], gave bands at (325, 355, 435) nm. These resulted bands are due to CT (t$_{2g}$ → π*) and CT (π →e$_g$). Its room temperature $μ_{eff}$ value of 5.2 B.M, typified the existence of O$_h$ configuration [20]. The buff electronic absorption spectrum of manganese-complex, [Mn (HL$_2$) (H$_2$O) Cl] gave three bands at (310, 355, 390) nm which assigned to π - π* and $^6A_{1g}$→$^4A_{1g}$ transitions. Its room temperature $μ_{eff}$ value of 5.1 B.M, typified the existence of O$_h$ configuration [21]. The yellow electronic absorption spectra for Nickel-complex [Ni (L$_2$)]. H$_2$O showed three bands at (325, 355, 445) nm due to charge transfer and $^3T_{1(F)}$→$^3T_{1(P)}$ transitions, So it has tetrahedral geometry further deduced from the $μ_{eff}$ value which equals 3.1 B.M, [22] and these results are in good agreement with the published work [23] that gave the $μ_{eff}$ values (3.42). The green copper complex [Cu (HL$_2$) (H$_2$O) Cl], exhibited bands at (325, 355, 430) nm. The latter broad bands are assigned to the ^2E_g → $^2T_{2g}$ (D) transition assignable to octahedral environment with room temperature $μ_{eff}$ values of 1.75 B.M [22]. These results are in good agreement with the published work [23] that determined $μ_{eff}$ values of (1.9). The yellow Zinc and Cadmium complexes exhibited bands which are assigned to ligand →metal charge transfer. Owing to the d^{10}- configuration of Zn (II) and Cd (II), no d-d transition could be observed and therefore, the stereochemistry around these metals in their complexes cannot be determined from ultraviolet and visible spectra [24]. However, by comparing the spectra of these complexes and those of similar environments, an octahedral structure was suggested for these complexes. Nujol mull electronic absorption spectra of Amoxicillin and its complexes are illustrated in Table 3 and Figure 2.

Table 3: Nujol mull electronic absorption spectra λ_{max} (nm), room temperature effective magnetic moment values (μ_{eff} 298°K) and geometries of Amoxicillin metal complexes

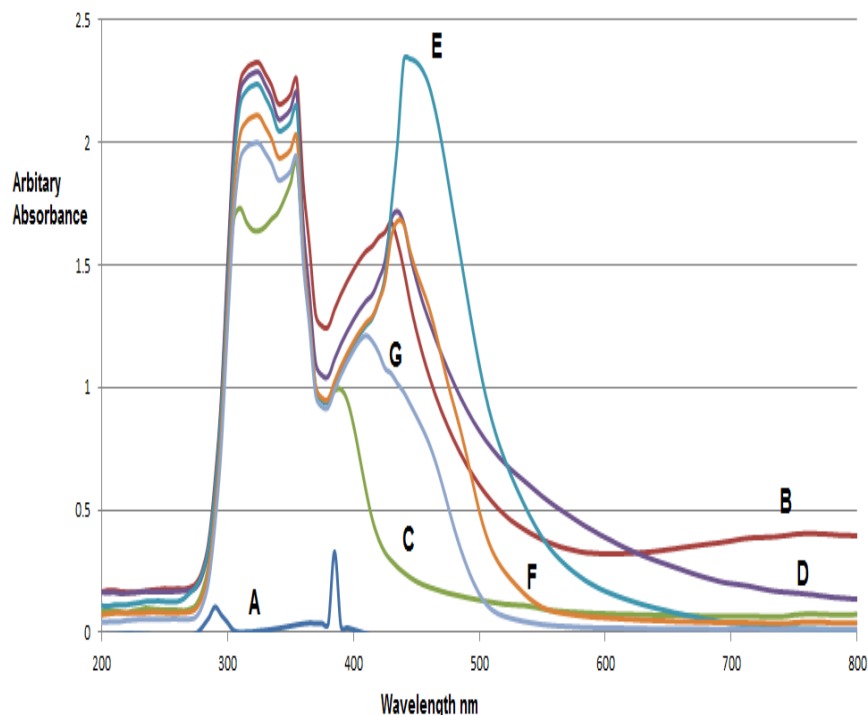| Complex	λ_{max} (nm)	μ_{eff}	Geometry
Amoxicillin (HL)	290, 385		
[Ni(L$_2$)].H$_2$O	325, 355, 445	3.1	T_d
[Fe (L$_2$) (H$_2$O) Cl]	325, 355, 435	5.2	O_h
[Cu (HL$_2$)(H$_2$O) Cl]	325, 355, 430	1.75	O_h
[Zn (HL)$_2$ (Cl)$_2$]	325, 355, 410	Diamagnetic	O_h
[Cd (HL$_2$) (H$_2$O) Cl]	325, 355, 435	Diamagnetic	O_h
[Mn (HL$_2$) (H$_2$O) Cl]	310, 355, 390	5.1	O_h

Figure 2: Nujol mull electronic absorption spectra of Amoxicillin and its complexes (A): Amoxicillin, (B) Cu complex, (C) Mn complex, (D) Fe complex, (E) Ni complex, (F) Cd complex and (G) Zn complex

Electron spin resonance of copper complex

The room temperature polycrystalline X-band ESR spectral pattern of [Cu (HL$_2$) (H$_2$O) Cl] complex, Figure (3) and Table (4) is Rhombic. It gave three peaks with g_1, g_2 and g_3 tensor values 2.66, 1.88 and 1.58, respectively in the trend of $g_1 > g_2 > g_3$. This goes in hormony with published work [25] for the five-coordinate Cu-(ATU)$_2$ complex and with published work [24] for the five-coordinate copper barbital complex with the formula Cu. H$_2$L$_3$.Cl complex. These complexes showed rhombic symmetry where g_1 = 2.56, 2.28, g_2 = 2.21, 2.14 and g_3 = 1.89, 1.96, respectively, due to disruption of local copper (II) environment. The calculated g_{av} value is (2.04). The value of the R of this complex typified the existence of (TBP) geometry of d_z^2 ground state, where R = 2.6 (i.e. >1).

Table 4: ESR values for Cu complex

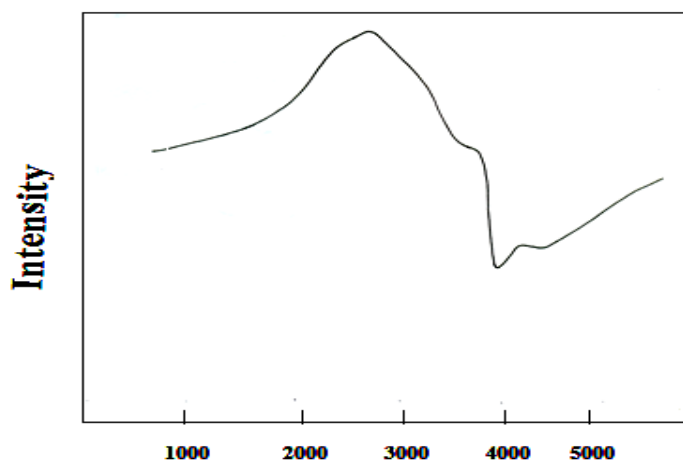| Complex	g_1	g_2	g_3	$\langle g \rangle$	R
[Cu(HL$_2$)(H$_2$O) Cl]	2.66	1.88	1.58	2.04	2.6

Figure 3: X-band ESR spectra of [Cu (HL₂)Cl(H₂O)]complex
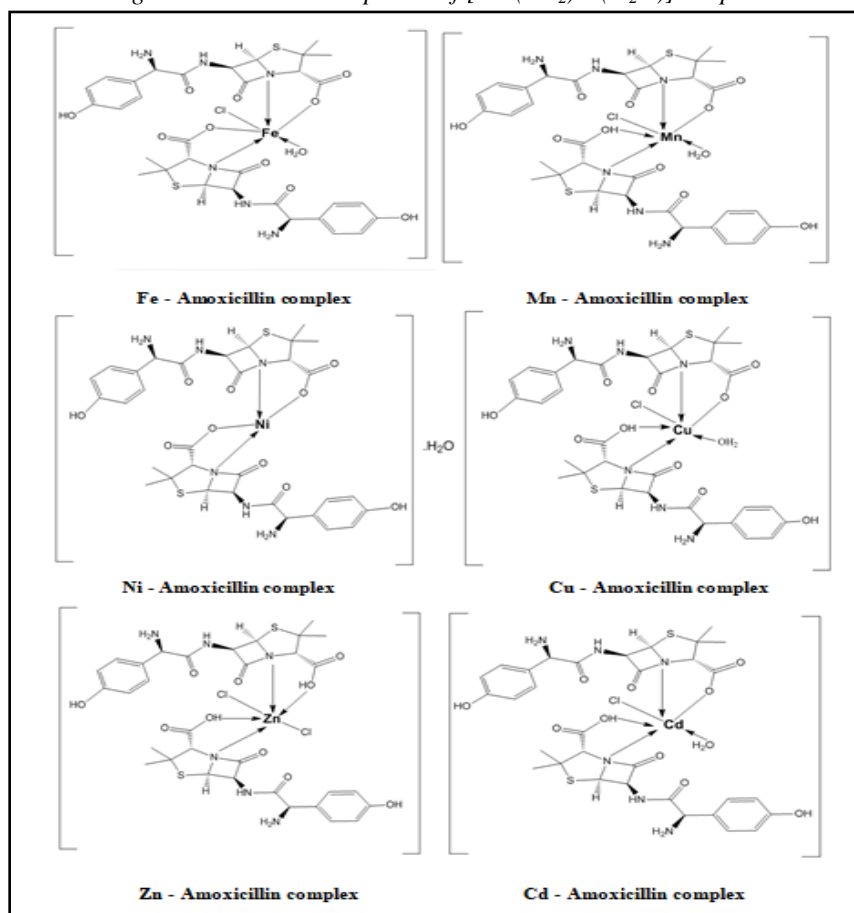
Figure 4: Proposed structures of Amoxicillin complexes

Biological activity

The data in Table (5), allowed the following observations and conclusions: All the investigated compounds have higher positive antibacterial activity compared to antifungal activity. [Cu (HL)₂ (H₂O)Cl] complex showed activity in the same range of Amoxicillin (HL) for Escherischia coli. It showed a relatively good activity higher than Amoxicillin (HL) for Staphyllococcus aureus and Bacillus subtilis. On the other hand, [Zn(HL)₂(Cl)₂] complex showed activity in the same range of Amoxicillin (HL) for Bacillus subtilis. It showed a relatively good activity higher than Amoxicillin (HL) for Escherischia coli.

Table 5: The antibictrial activity of the free ligands and their complexes against some reference strains expressed in absolute activity (AU)

Compound	Staphyllococcus aureus		Bacillus subtilis		Pseudomonas aeruginosa		Escherischia coli		Candida albicans	
	Control	**Cpd.**	**Control**	**Cpd.**	**Control**	**Cpd.**	**Control**	**Cpd.**	**Control**	**Cpd.**
[Cu(HL)$_2$(H$_2$O)Cl]	9	45	9	15	9	9	9	20	9	9
[Zn(HL)$_2$(Cl)$_2$]	9	34	9	13	9	9	9	21	9	9
Amoxicillin(HL)	9	40	9	13	9	9	9	20	9	9
Ciprofloxacin	9	30	10	30	9	30	9	30	-	-
Clotrimazole	-	-	-	-	-	-	-	-	9	18
DMSO	-	-	-	-	-	-	-	-	-	-

(-) = No activity

Most of the metal complexes have higher activity than the free ligands which explained on the bases of chelation theory. The cell permeability of the lipid membrane that surrounds the cell favours the passage of lipid soluble materials only on the basis that liposolubility is the most important factor that controls antimicrobial activity. On chelation, the polarity of the metal ion is reduced due to the high overlap of the ligand orbitals and partial sharing of the metal ion positive charge with the donor groups. This increases the delocalization of p- and d-electrons and it enhances the lipophilicity of the complex. The increased lipophilicity also enhances the penetration of these complexes into lipid membranes and blocking the metal binding sites on the enzymes of the microorganism [26, 27], and these results go in hormony with published work [28, 29] that say polarity of the metal ions is reduced on chelation. On the other hand, Zinc complex of amoxicillin [Zn(HL)$_2$(Cl)$_2$] showed decreased antibacterial activities when compared to those of the corresponding ligand for Staphyllococcus aureus. This is due to the loss of some essential pharmacophoric moieties caused by coordination with the metal ion. The sites used for dative bonding with the central metal ion are no longer available for binding with the biological receptors in the microorganisms. The complexed form of the drug is not capable of such chelation since the chelation sites are already occupied. A deviation from the optimal lipophilicity due to increased aqueous solubility can also account for the activity [30]. Comparison between biological activity of Amoxicillin and its metal complexes is illustrated in Fig. 5.
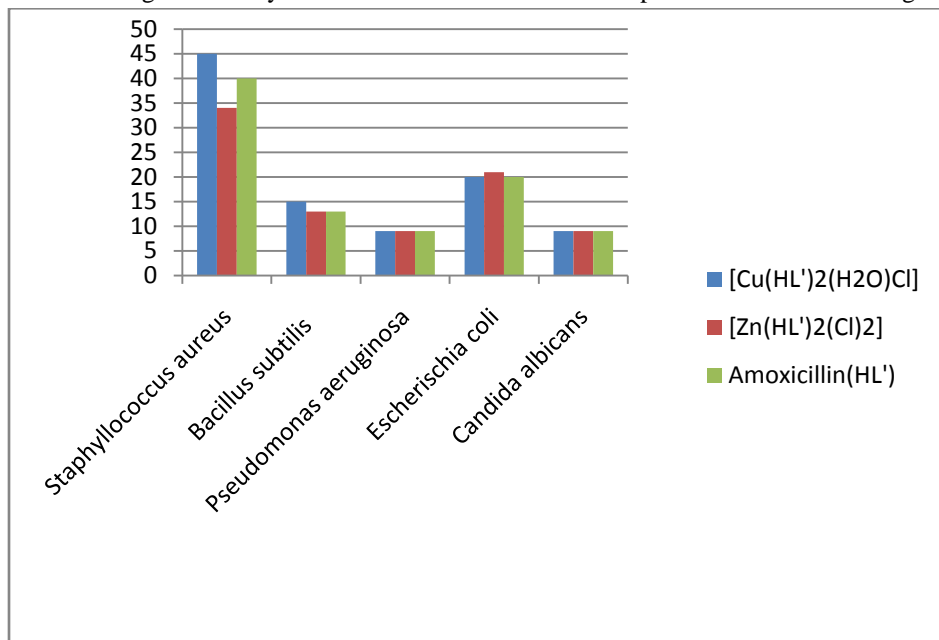

Figure 5: Comparison between the antibacterial activity of Amoxicillin and its complexes against some reference strains

Thermal analysis

The thermal behavior of some biologically active compounds had been reported from Masoud et al[19, 31, 32].The TGA and DTA data of Amoxicillin and its complexes, Figures (6 - 12) and Table (6), allowed the following observations and conclusions:

From DTA data, Amoxicillin decomposition showed four bands at 83.8, 158, 263.7 and 636.8 ℃ with activation energies 165.98, 307.58, 88.05 and 425.1 KJ/mole with orders 0.98, 1.03, 1.78 and 2.09, respectively indicating first order reaction for the first and second peak and second order for third and fourth peak. The first and second peak were Endothermic but the third and fourth peak were Exothermic. The TGA data confirmed these results which gave four decomposition steps. Amoxicillin ligand loses mass between 35°C and 170°C, corresponding to nearly 12.6 % of the total mass, followed by considerable decomposition up to 700°C nearly 84 % of the total mass.
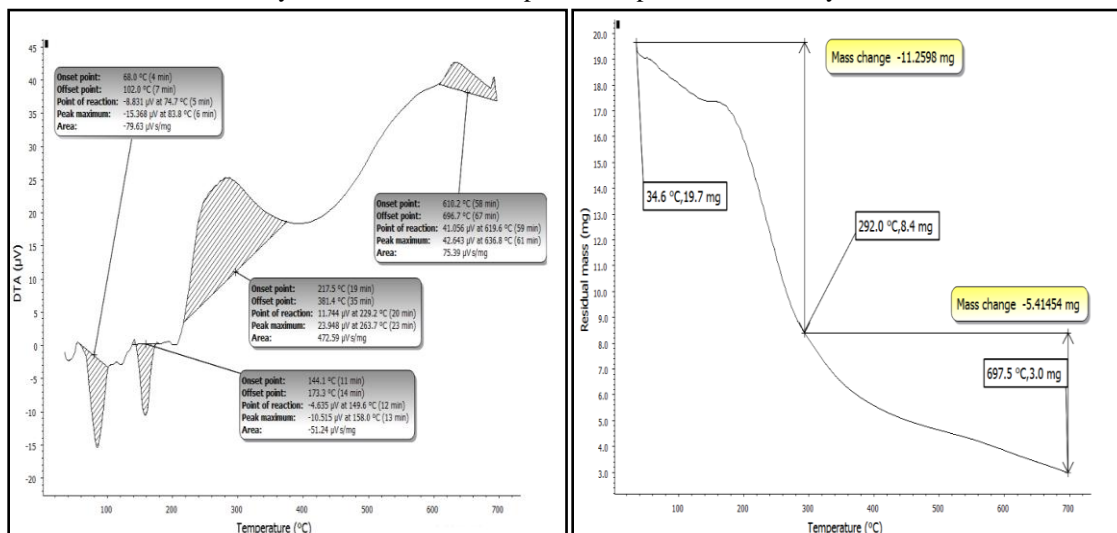
Figure 6: DTA and TGA of Amoxicillin ligand

The DTA sheet of Amoxicillin - Cadmium complex [Cd (HL$_2$) (H$_2$O) Cl] showed three peaks at 194.8, 419.4 and 653.6 °C with activation energies of 54.7, 36.7 and 223.8 kJ/mole, their orders of reactions were 1.26, 1.26 and 1.35, respectively. All the data suggested first order reactions. The first two peaks were Endothermic but the third peak was Exothermic. The TGA data confirmed these results which gave three decomposition steps. The [Cd (HL$_2$) (H$_2$O) Cl] complex decomposes nearly 26.4 % of the total mass up to temperature 700°C.

Figure 7: DTA and TGA of [Cd (HL$_2$) (H$_2$O) Cl] complex

The DTA sheet of Amoxicillin - Nickel complex [Ni (L_2)].H_2O, gave well-defined three peaks at 101.7, 226.1 and 452.9 °C with activation energies of 16.42, 71.46 and 94.59 kJ/mole and their orders were 1.32, 2.09 and 1.37. All peaks were of the endothermic type. The first and third peak were of the first order type but the second peak was of the second order. The TGA data confirmed these results which gave three decomposition steps. [Ni(L_2)].H_2O complex decomposes nearly 57.6 % of its weight till 700 °C.
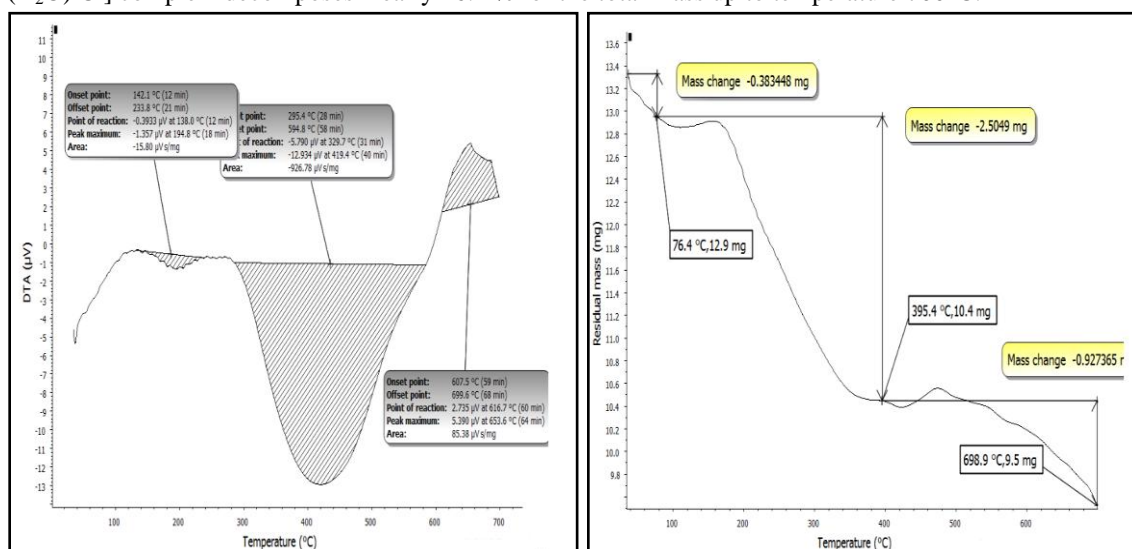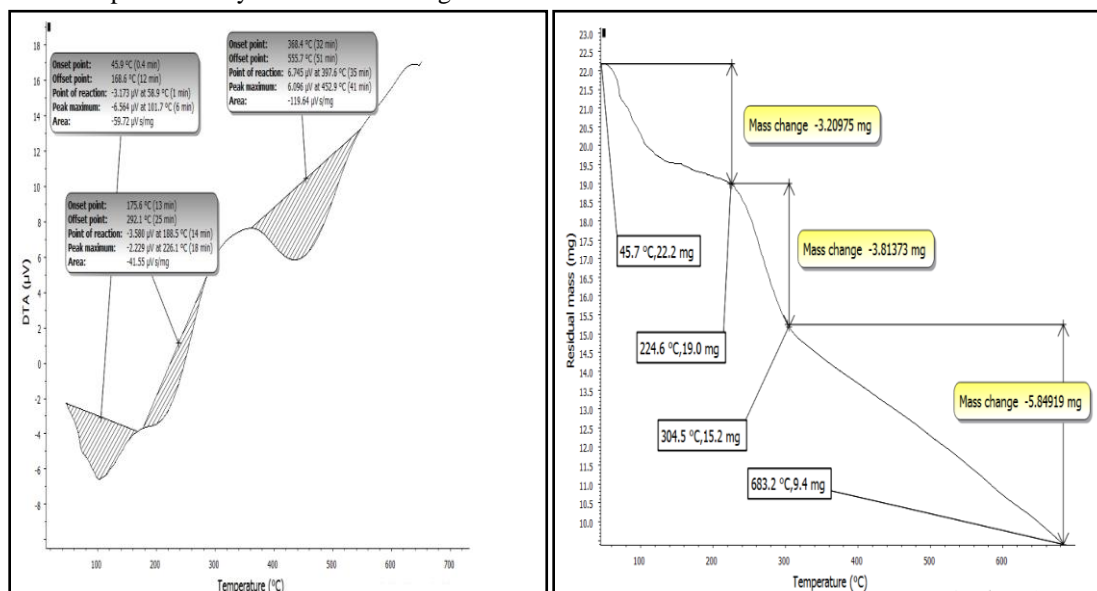

Figure 8: DTA and TGA of [Ni (L_2)].H_2O complex

The DTA sheet of Amoxicillin - Cupper complex [Cu (HL_2) (H_2O) Cl] showed three peaks at 80.8, 242 and 497.5 °C with activation energies of 33.37, 57.05 and 22.11 kJ/mole, their orders of reactions were 1.76, 3.07 and 0.67, respectively. The data typified first order reaction for the third peak, second order reaction for first peak and third order reaction for second peak. All resulted peaks were Endothermic in nature. The TGA data confirmed these results which gave three decomposition steps and the [Cu (HL_2)(H_2O) Cl] complex decomposes nearly 50.6 % of its weight till 700 °C.
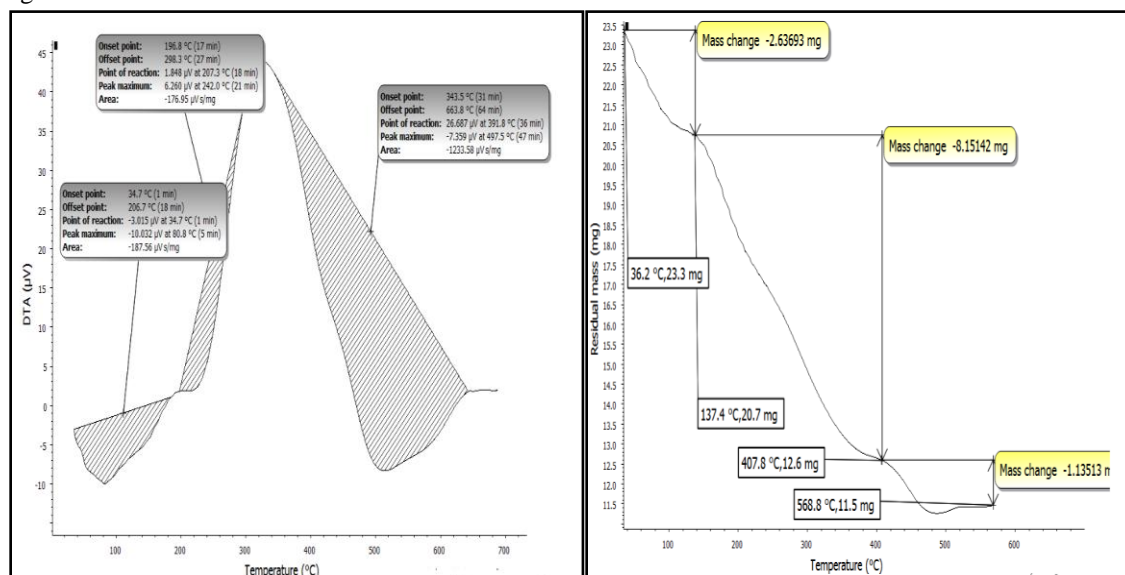
Figure 9: DTA and TGA of [Cu (HL_2) (H_2O) Cl] complex

From DTA sheet of [Fe (L$_2$) (H$_2$O) Cl] complex, four peaks were observed at 60, 184.2, 398.7 and 637.5 °C with activation energies of 31.41, 88.26, 33.78 and 366.2 kJ/mole, their reaction orders were 1.26, 1.39, 1.23 and 1.49 which typified first order reactions. The first three peaks were Endothermic but the last one was Exothermic. The 4 peaks were merged in three decomposition steps in which the complex decomposed nearly 49.5 % of its weight till 700°C.
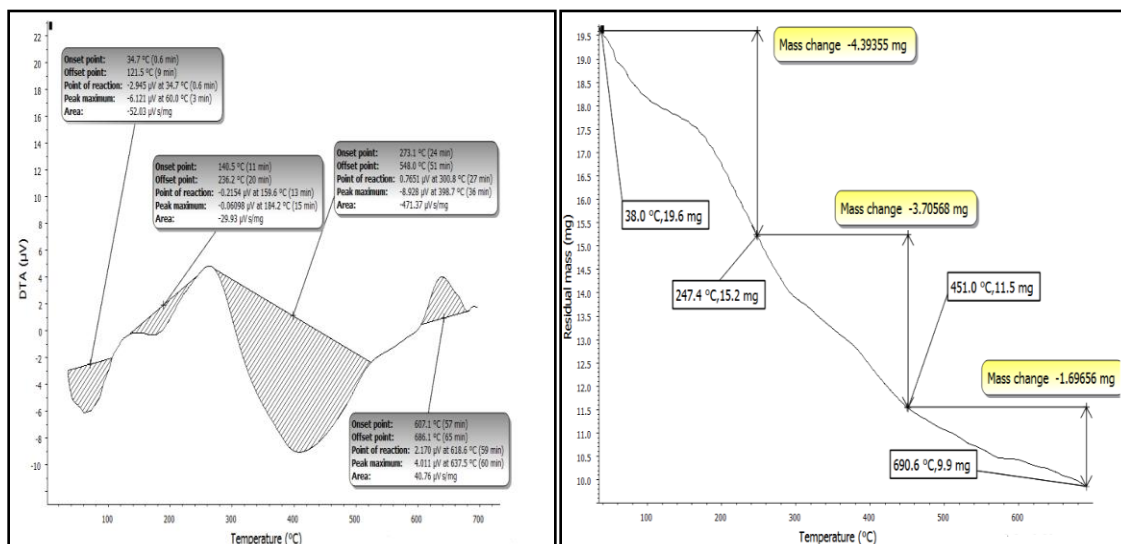
Figure 10: DTA and TGA of [Fe (L$_2$) (H$_2$O) Cl] complex

The DTA data of [Zn (HL)$_2$ (Cl)$_2$] complex, gave four peaks at 113.4, 223.5, 412 and 628.1 °C with activation energies of 26.56, 195.6, 52.05 and 109.16 kJ/mole and their orders were 1.37, 1.2, 1.23 and 1.03, respectively. All peaks were exothermic except the third one was endothermic in nature. All the orders of reactions were of the first type, The 4 peaks were merged in three decomposition steps in TGA sheet in which complex decomposed nearly 31.7 % of its total mass up to the same temperature (700°C).
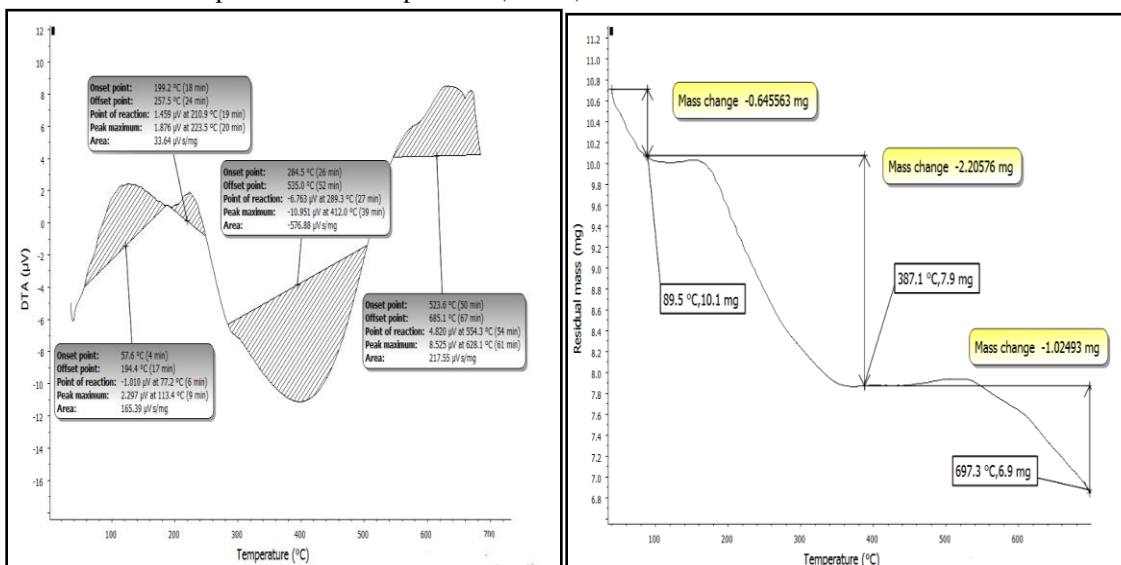
Figure 11: DTA and TGA of [Zn (HL)$_2$ (Cl)$_2$] complex

The DTA data of [Mn (HL$_2$) (H$_2$O) Cl] complex, gave four peaks at 54.2, 124.4, 386.1 and 644.9°C with activation energies of 167.85, 86.8, 147.79 and 298.35 kJ/mole and their orders were 2.36, 2.03, 1.59 and 1.26 , respectively. The first and the third peak were endothermic but the second and the fourth peak were exothermic. All the orders of reactions were of the second type except the last one is of the first type. The 4 peaks were merged in three

decomposition steps in TGA sheet which illustrated that the Manganese complex decomposes nearly 42.9 % till 700°C.

Figure 12: DTA and TGA of [Mn (HL₂) (H₂O) Cl] complex

All these results revealed that the prepared complexes are more thermally stable than the ligands.

Table 6: DTA analysis of Amoxicillin and its metal complexes

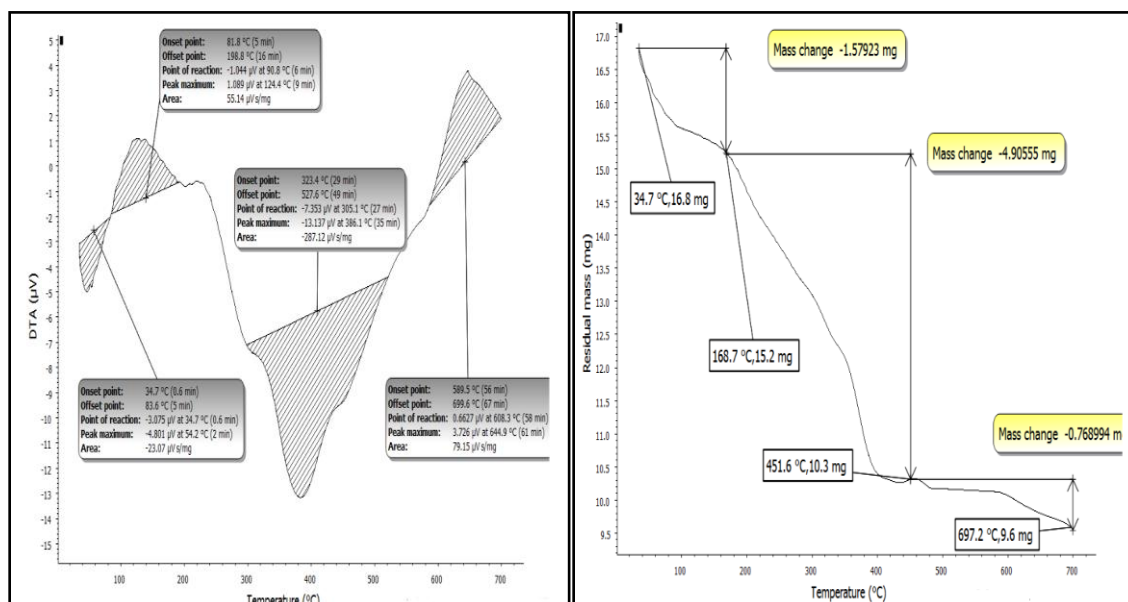|	Type	Tm (°C)	E_a (kJ mol⁻¹)	n	α_m	$\Delta S^{\#}$ (kJ K⁻¹ mol⁻¹)	$\Delta H^{\#}$ (kJ mol⁻¹)	Z (S⁻¹)	Temp. (°C) TGA	Wt. Loss % Calc.	Found	Suggested Assignment
Amoxicillin	Endo	83.8	165.98	0.98	0.64	-0.27	-22.2	0.237	34 – 180 °C	13.7	12.9	**Dehydration of 3H₂O**
	Endo	158	307.58	1.03	0.63	-0.27	-42.8	0.233	180 – 292 °C	43.65	43.0	**Loss of C₆H₅OH, NH₃, CH₃CONH, H₂O**
	Exo	263.7	88.05	1.78	0.52	-0.29	-76.4	0.04	292 – 560 °C	22.33	19.6	**Loss of HC(CH₃)₂CH₂CO**
	Exo	636.8	425.1	2.09	0.49	-0.29	-185.5	0.08	560 – 697 °C	5.07	9.8	**Loss of CH₃CONH₂**
[Cd (HL₂)(H₂O) Cl]	Endo	194.8	54.7	1.26	0.59	-0.29	-56.24	0.034	34 – 76 °C	3.73	3.46	**Loss of 2NH₃**
	Endo	419.4	36.7	1.26	0.59	-0.3	-127.8	0.01	76 – 395 °C	18.66	20.3	**Dehydration of H₂O, Loss of HCl, 2C₅H₅OH**
	Exo	653.6	223.8	1.35	0.58	-0.3	-194.19	0.04	395 – 699 °C	6.7	6.25	**Loss of 2C₂H₆**
[Ni (L₂)]. H₂O	Endo	101.7	16.42	1.32	0.58	-0.29	-29.28	0.019	46 – 225 °C	14.4	15.9	**Dehydration of H₂O, Loss of 2NH₃, 2CH₃CH₂OH**
	Endo	226.1	71.46	2.09	0.49	-0.29	-65.33	0.038	225 – 305 °C	17.1	16.4	**Loss of 2C₅H₇**
	Endo	452.9	94.59	1.37	0.57	-0.3	-135.04	0.025	305 – 683 °C	26.1	27.3	**Loss of 4CH₃NHCO,**
[Cu (HL₂) (H₂O) Cl]	Endo	80.8	33.37	1.76	0.53	-0.28	-22.48	0.049	36 – 137 °C	11.16	10.03	**Dehydration of H₂O, Loss of 2NH₃, HCl**
	Endo	242	57.05	3.07	0.42	-0.29	-70.65	0.028	137 – 408 °C	34.76	35.18	**Loss of 2C₆H₅OH, 2 CH₃CONH₂**
	Endo	497.5	22.11	0.67	0.7	-0.31	-155.13	0.005	408 – 567 °C	4.72	6.14	**Loss of 2CO**
[Fe (L₂) (H₂O) Cl]	Endo	60	31.41	1.26	0.59	-0.27	-16.42	0.063	38 – 247 °C	22.44	22.37	**Dehydration of H₂O, Loss of 2NH₃, HCl, Loss of 2CH₃CHOHCH₃**

	Endo	184.2	88.26	1.39 0.57	-0.28	-52.27	0.058			
	Endo	398.7	33.78	1.23 0.59	-0.30	-121.4	0.01	247 – 451 °C	18.9	19.6	Loss of 2CH$_3$CHCH$_3$CH$_2$CHO
	Exo	637.5	366.2	1.49 0.56	-0.29	-186.5	0.069	451 – 691 °C	8.16	9.78	Loss of 2NH$_3$, 2CO
[Zn (HL)$_2$ (Cl)$_2$]	Exo	113.4	26.56	1.37 0.57	-0.28	-32.4	0.03	36 – 90 °C	6.48	8.4	Loss of 2HCl
	Exo	223.5	195.6	1.2 0.6	-0.28	-62.67	0.1	90 – 387 °C	20.37	18.0	Loss of 2C$_5$H$_4$OH
	Endo	412	52.05	1.23 0.59	-0.3	-124.2	0.015	387 – 697 °C	9.26	9.9	Loss of 2CH$_3$CH$_2$NH$_2$
	Exo	628.1	109.16	1.03 0.63	-0.3	-189.9	0.02			
[Mn(HL$_2$)(H$_2$O) Cl]	Endo	54.2	167.85	2.36 0.47	-0.26	-13.99	0.368	34 – 169 °C	9.5	10.0	Dehydration of H$_2$O, Loss of 2NH$_3$, HCl
	Exo	124.4	86.8	2.03 0.5	-0.28	-34.5	0.084			
	Endo	386.1	147.79	1.59 0.54	-0.29	-112.67	0.046	169 – 452 °C	29.16	28.6	Loss of 2C$_6$H$_5$OH, 2CO
	Exo	644.9	298.35	1.26 0.59	-0.29	-189.92	0.056	452 – 697 °C	4.16	5.13	Loss of 2CH$_3$

The change of entropy, $\Delta S^{\#}$, values for all complexes, Tables (6), are nearly of the same magnitude and lie within the range of (-0.26) to (-0.31) kJk^{-1}mole^{-1} for all prepared Amoxicillin complexes. The values of the heat of transformation, $\Delta H^{\#}$ lie within the range of (-13.99) to (-194.19) kJk^{-1}mole^{-1}. The negative values of activation entropies ($\Delta S^{\neq}$) indicated a more ordered activated complex than the reactants and the reactions are slow. It also indicated that the complexes are formed spontaneously. The negative values of activation enthalpy ($\Delta H^{\neq}$) show that the decomposition process is exothermic [33]. The calculated values of the collision number, Z showed a direct relation to E$_a$ [34]. It lied in the range of (0.005 -0.368). The position of the peak is defined by the peak temperature, T$_m$, at which the peak is maximum or minimum. Also the values of the decomposed substance fraction, α_m, at the maximum development of the reaction were calculated [32]. It is of nearly the same magnitude and lies within the range (0.42- 0.7).

Based on these calculations, the ln ΔT versus $10^3/T$ plots for all complexes, Figures (13), gave straight lines from which the activation energies were calculated according to the methods of Piloyan [35]. The order of chemical reactions (n) was calculated via the peak symmetry method [36]. In all experiments the heating rate is 10°C/min.

Computational Studies and Molecular Modeling of Amoxicillin metal complexes

The computational study of Amoxicillin and its metal complexes is presented here using Semi emperical (PM6) and density functional theory (DFT) in its hybrid form B3LYP. The geometries of the complexes are described by the quantum-chemical approach using input coordinates obtained from the previously data. The complexes were optimized in the gaseous phase. Comparison between the optimized parameters of the primary coordination sphere of complexes and the primary ligands was done. Calculations of the energy gaps of frontier orbitals (HOMO-LUMO) was done, Charge transfer was studied for the ligand and metal complexes and UV Excitation Energies were compared with the experimental data [37].

HOMO-LUMO analyses and spectroscopic calculations were performed on the optimized geometries. The molecular modeling data including charges, bond lengths, bond angles and dihedral angles of the parent ligand **Amoxicillin and its metal complexes** are based on neglecting the possibility of hydrogen bonding. All DFT computations were carried out starting from the supposed structure as input geometry [38].
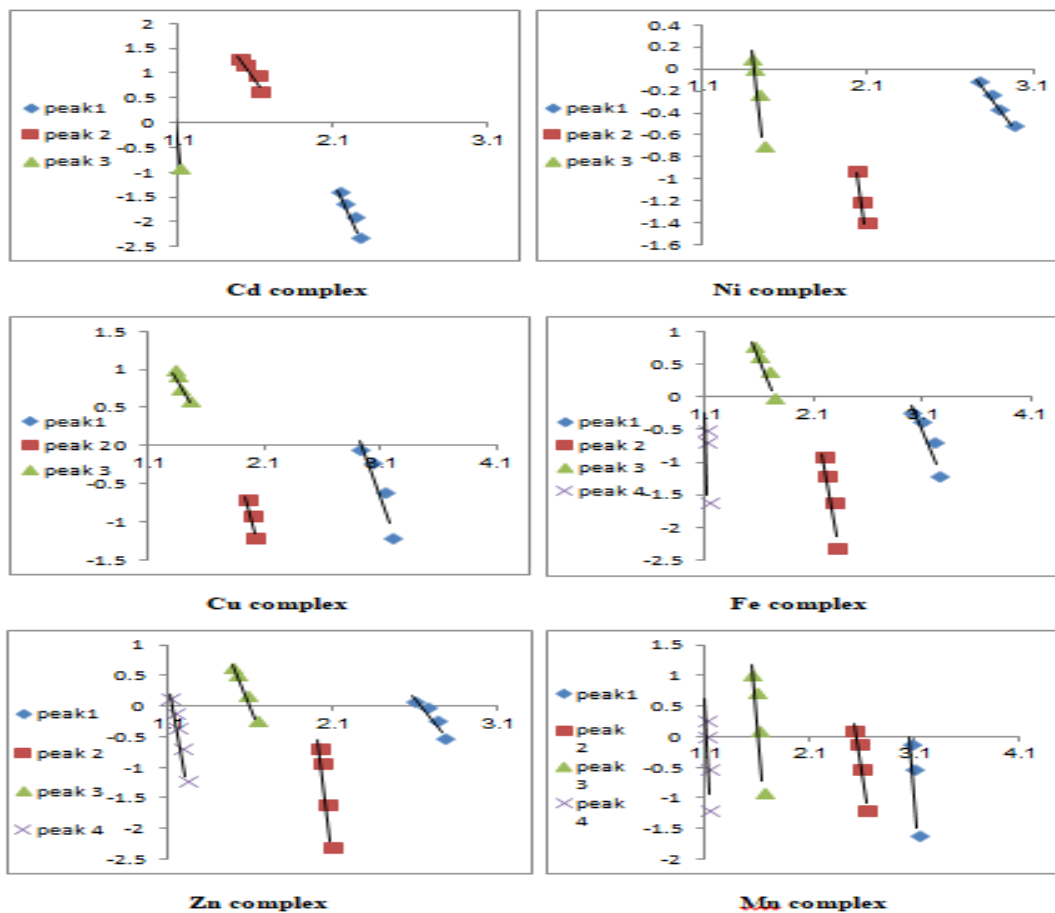
Figure 13: lnΔT against $10^3/T$ relations for Amoxicillin complexes

Molecular modeling and Optimization of Amoxicillin and its metal complexes Using Semiempirical (PM6) and DFT-B3LYP /LANL2DZ basis sets:

From Experimental data, Fe, Cu, Cd and Mn complexes have the same octahedral strucures [$ML_2(H_2O)Cl$] , So we computationally studied only one complex of them in detail. Also, we studied Zn complex with [ML_2Cl_2] octahedral structure and Ni complex [ML_2] tetrahedral strucure.

A- Geometry optimization

The results obtained from the geometry optimizations carried out by the PM6 and DFT-B3LYP methods for Amoxicillin and its metal complexes are listed in (Table 7) in comparison with each other. The numeration of atoms and directions of bond unit vectors used in the calculations for modelling of Amoxicillin and its metal complexes are shown in (Figures 14 - 17).

Amoxicillin ligand
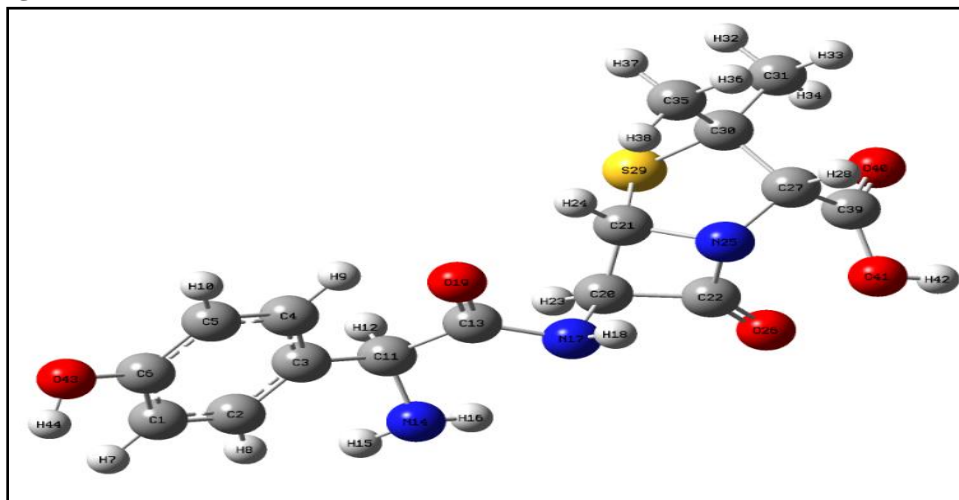
Figure 14: The optimized molecular structure of Amoxicillin using DFT/B3LYP/LAN2DZ

Upon complexation of 2 molecules of Amoxicillin ligand with one metal atom (Cu, Zn and Ni), the R of C21—N25 is unchanged in Cu and Zn complexes but it is elongated by about (0.0195 – 0.0129) Å in Ni complex. The R of C22—N25 is shortened by about (0.0268 – 0.0217) Å in Cu complex, and it is also shortened by about (0.0356 – 0.0324) Å in Zn complex but, it is elongated by about (0.0581 – 0.0157) Å in Ni complex. The R of N25—C27 is unchanged in Cu and Zn complexes but it is elongated by about (0.0411 – 0.0115) Å in Ni complex. Also, the R of C39—O41 is shortened by about (0.042 – 0.0039) Å in Cu complex, by about (0.0231 – 0.0001) Å in Zn complex, and by about (0.054 – 0.076) Å in Ni complex. While the R of O41— C42 is elongated by about (0.0327-0.0538) Å in Cu complex and by about (0.0169- 0.0402) Å in Zn complex but this bond isn't found in Ni complex. The other bond lengths within the amoxicillin moiety are slightly affected or unchanged.

The bond angles within the amoxicillin moiety are slightly affected by complexation (increased or decreased by about 5˚) as illustrated in Table 7.

Amoxicillin –Cupper complex

The Cupper complex ends up with an octahedral geometry with one chlorine atom, one oxygen of water molecule, two endo oxygen atoms and two endo nitrogen atoms in the initial amoxicillin ligand, (Figure 15). The optimized geometric bond lengths R, bond angles A, and dihedral angles D of the complex are affected by the method used in the calculations, (Table 7). The calculations indicated that the Cu—Cl bond distance decreased as the method changed in order of DFT> PM6 and its calculated value is in the range of (2.344 - 2.1289) Å. The trend is true for R of the Cu—O41 and Cu—O83 bonds. Their calculated values are in the range of (3.9502 - 2.0598) Å and (1.978 - 1.8793) Å, respectively. For Cu—N25 and Cu—N67, the trend is only true for Cu—N25 which has calculated values in the range of (4.5239 - 3.5558) Å, but for Cu—N67, the bond distance increased in order of DFT< PM6 and the calculated values are in the range of (3.5506 - 3.752) Å. This trend is also true for Cu–OH$_2$, its bond distance is in the range of (1.9739-2.1166) Å.

The calculated A values of the angles O83–Cu–O85, O85–Cu–N25, N25–Cu–O41, O41– Cu–Cl84, Cl84–Cu–N67 and N67–Cu–O83 bond angles using the different methods (DFT and PM6) were found to be in the ranges of (81.7917 – 78.1593)˚, (83.1682 – 111.3137)˚, (38.0046 – 53.8461)˚, (49.4506 – 83.6243)˚, (130.1122 – 86.6976)˚ and (51.0673 – 41.0377)˚, respectively. It was shown from calculated A values for the angles around the centre metal atom that the complex is distorted octahedral, (Figure 15).

From the calculated D values for C81–O83–Cu–N25, C64–N67–Cu–O85, C64–N67–Cu–O83, C63–N67–Cu–O83, C62–C64–N67–Cu and C20–C22–N25–Cu, The values for this angle are (-176.924 – -178.73)˚, (173.6993 – 156.2319)˚, (-166.149 – -172.441)˚, (177.9429 – 166.9277)˚, (-174.678 – -170.886)˚ and (-174.455 –

175.9174)˚using DFT and PM6 basis sets, respectively. This indicates that these atoms are predicted to be nearly planar with the metal atom. Also, the D values for C20–C21–N25–Cu, O26–C22–N25–Cu and O68–C64–N67–Cu are (9.9413 – 8.6197)˚, (0.9959 – -6.349)˚, (3.5197 –11.1512)˚ using DFT and PM6 basis sets, respectively which have no deviation from planarity.
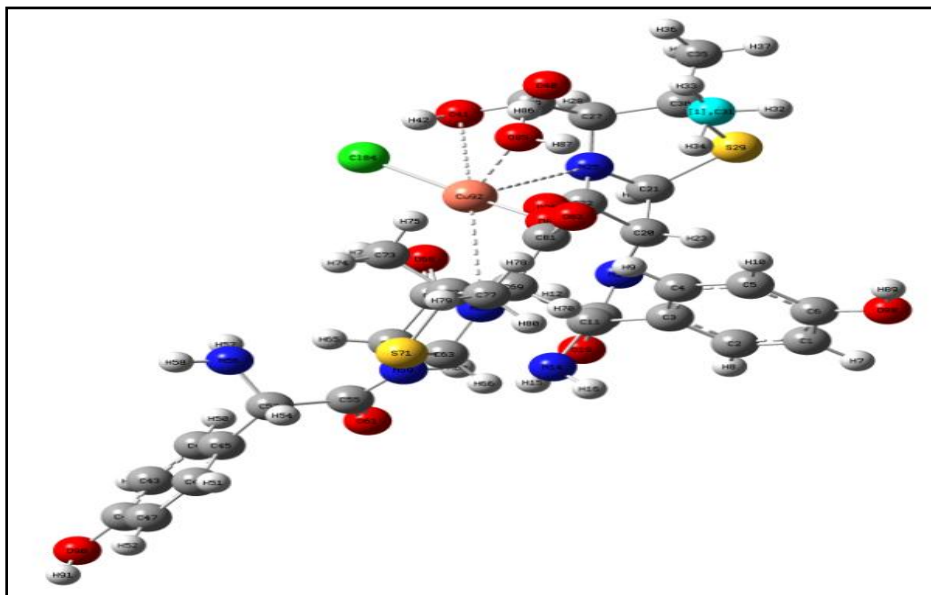

Figure 15: The optimized molecular structure of Amoxicillin-Cu complex using DFT/B3LYP/LAN2DZ

Amoxicillin –Zinc complex

The Zinc complex ends up with an octahedral geometry with two chlorines, two endo oxygen atoms and two endo nitrogen atoms in the initial amoxicillin ligand, (Figure 16). The optimized geometric bond lengths R, bond angles A, and dihedral angles D of the complex are affected by the method used in the calculations. The calculations indicated that the two Zn—Cl bond distances are nearly equivalent and differs only by about 0.062 Å using the same method (DFT). The R of the Zn—Cl84 and Zn—Cl85 bond distances decreased as the method changed in order of DFT> PM6 and their calculated values are in the range of (2.373 - 2.221) Å. The trend is true for R of the Zn—O41 and Zn—O83 bonds. Their calculated values are in the range of (2.974 - 2.371) Å and (3.4727 – 2.3894) Å, respectively. For Zn—N25 and Zn—N67, the trend is also true and the calculated values are in the range of (4.1034 - 3.8483) Å and (3.9839 - 3.7663) Å, respectively.

The calculated A values of the angles Cl85–Zn–N25, N25–Zn–O41, O41–Zn–Cl84, Cl84– Zn–O83, O83–Zn–N67 and N67–Zn–Cl85 bond angles using the different methods (DFT and PM6) were found to be in the ranges of (98.578 – 76.1812)˚, (43.304 – 47.9201)˚, (67.0675 – 78.2885)˚, (81.8855 – 84.0045)˚, (47.1878 – 48.2682)˚ and (70.0202 – 82.181)˚, respectively. It was shown from calculated A values for the angles around the centre metal atom that the complex is distorted octahedral, (Figure 16).

From the calculated D values for C21–N25–Zn–Cl, C22–N25–Zn–O41, C62–C64–N67–Zn, C63–N67–Zn–O83, C64–N67–Zn–O83, C69–N67–Zn–N25 and C81–O83–Zn–N25, The values for this angle are (179.7247 – - 171.084)˚, (175.4859 – -157.341)˚, (162.7728 – 176.1832)˚, (-165.714 – 174.5855)˚, (169.8543 – -179.163)˚, (167.4743 – 169.9367)˚ and (178.0222 – 163.7235)˚using DFT and PM6 basis sets, respectively. This indicates that these atoms are predicted to be nearly planar with the metal atom Zn.
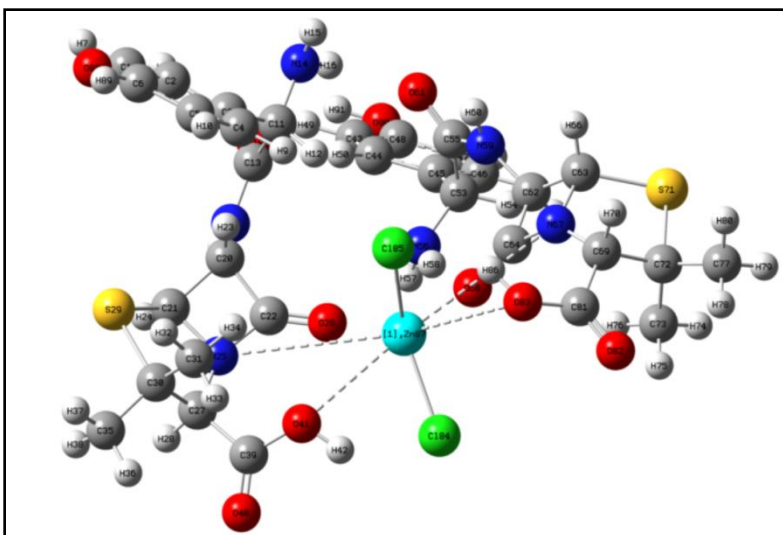
Figure 16: The optimized molecular structure of Amoxicillin-Zn complex using DFT/B3LYP/LAN2DZ

Amoxicillin - Ni complex

The Nickel complex ends up with a tetrahedral geometry with two endo oxygen atoms and two endo nitrogen atoms in the initial amoxicillin ligand, (Figure 17). The optimized geometric bond lengths R, bond angles A, and dihedral angles D of the complex are affected by the method used in the calculations, (Table 7). The calculations indicated that the R of the Ni—O41 and the Ni—O82 bond distances decreased as the method changed in order of DFT> PM6 and their calculated values are in the range of (1.8572 – 1.8519) Å and (1.8743– 1.8604) Å, respectively. The trend is true for R of Ni—N25 and R of Ni—N25 which are in the range of (2.1523 – 1.9376) Å and (2.0669– 1.9351) Å, respectively.
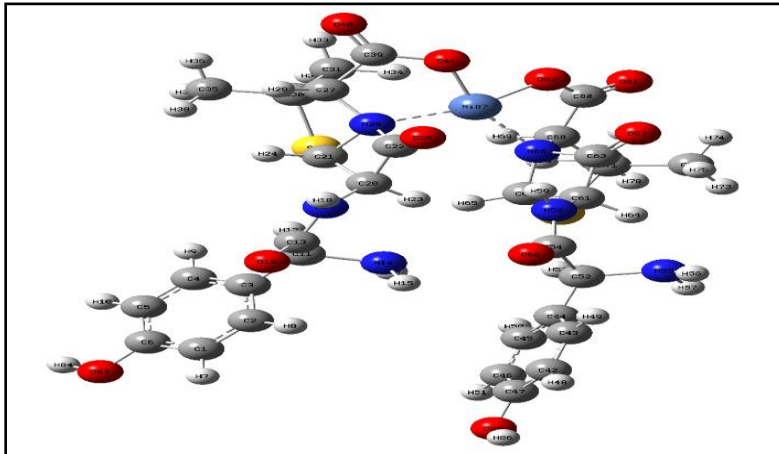
Figure 17: The optimized molecular structure of Amoxicillin Ni complex using DFT/B3LYP/LAN2DZ

The calculated A values of the angles O41–Ni–O82, O82–Ni–N66, N66– Ni –N25 and N25–Ni–O41 bond angles using the different methods (DFT and PM6) were found to be in the ranges of (84.7979 – 80.1362)°, (82.2504 – 84.2874)°, (112.4471– 109.7756)° and (82.1022 – 85.6303)°, respectively. It was shown from calculated A values for the angles around the centre metal atom that the complex is distorted tetrahedral, (Figure 17).

From the calculated D values for Ni–N66–C68–C71, C62–N66–Ni–O82 and O81–C80–O82–Ni, The values for this angle are (177.3121– -179.993)°, (-170.724 – 179.7863)° and (175.8076– 162.8191)°using DFT and PM6 basis sets, respectively. This indicates that these atoms are predicted to be nearly planar with the Nickel metal atom. Also, the D values for N68–C80–O82–Ni and C62–N66–Ni–N25 are (-1.0654– -18.264)°and (0.4814 – -4.2502)° using DFT and PM6 basis sets, respectively which have no deviation from planarity.

Table 7: The optimized geometry Parameters, bond length (R), bond angle (A) and dihedral angles (D) of Amoxicillin and its metal complexes calculated by the PM6 and DFT-B3LYP /LANL2DZ methods

Bond length (angestrom)								
Coordinates	**Amoxicillin**		**Cu Complex**		**Zn complex**		**Ni complex**	
	DFT	PM6	DFT	PM6	DFT	PM6	DFT	PM6
R(21,25)	1.4853	1.5028	1.4776	1.5065	1.4872	1.5028	1.5048	1.5157
R(22,25)	1.415	1.4613	1.3882	1.4396	1.3794	1.4289	1.4731	1.477
R(25,27)	1.4634	1.4774	1.4694	1.4704	1.4685	1.4677	1.5045	1.4889
R(39,41)	1.386	1.3723	1.344	1.3884	1.3629	1.3722	1.332	1.2963
R(41,42)	0.9848	0.9974	1.0175	1.0512	1.0017	1.0376	-	-
R(67,69) ≡ R(66,68)	1.4634	1.4774	1.4665	1.4776	1.4764	1.4763	1.5193	1.5059
R(64,67) ≡ R(63,66)	1.415	1.5028	1.3755	1.4436	1.3795	1.4469	1.516	1.5256
R(63,67) ≡ R(62,66)	1.4853	1.5028	1.4852	1.4989	1.4941	1.5084	1.5342	1.5239
R(81,83) ≡ R(80,82)	1.386	1.3723	1.3254	1.2981	1.3596	1.39	1.3347	1.2972
(M-N)1 bond R(25,92) ≡ R(25,87)	-	-	4.5239	3.5558	4.1034	3.8483	2.1523	1.9376
(M-O)1 bond R(41,92) ≡ R(41,87)	-	-	3.9502	2.0598	2.974	2.3711	1.8572	1.8519
(M-Cl)1 bond R(84,92) ≡ R(84,87)	-	-	2.344	2.1289	2.311	2.221	-	-
(M-O)H$_2$ R(85,92)	-	-	1.9739	2.1166	-	-	-	-
(M-Cl)2 bond R(85,87)	-	-	-	-	2.3731	2.2604	-	-
(M-O)2 bond R(83,92)≡R(83,87)≡R(82,87)	-	-	1.978	1.8793	3.4727	2.3894	1.8743	1.8604
(M-N)2 bond R(67,92)≡R(67,87)≡ R(66,87)	-	-	3.5506	3.752	3.9839	3.7663	2.0669	1.9351
Bond Angles (degree)								
A(21,25,92) ≡ A(21,25,87)	-	-	136.9788	145.7719	129.9321	126.0934	124.4474	131.2534
A(22,25,92) ≡ A(22,25,87)	-	-	41.9418	53.2533	38.0169	42.8761	105.2781	87.5163
A(27,25,92) ≡ A(27,25,87)	-	-	96.2309	91.1616	105.0294	91.2314	98.6375	99.8489
A(39,41,92) ≡ A(39,41,87)	-	-	81.4975	135.9218	116.615	142.7778	118.0842	105.379
A(42,41,92) ≡ A(42,41,87)	-	-	50.103	103.6887	77.6507	99.0446	-	-
A(63,67,92)≡A(63,67,87)≡A(62,66,87)	-	-	147.7456	143.1401	137.5331	144.7659	133.4925	138.5942
A(64,67,92)≡A(64,67,87)≡A(63,66,87)	-	-	53.9763	51.3389	45.4764	52.8902	102.7183	107.7842
A(69,67,92)≡A(69,67,87)≡A(68,66,87)	-	-	89.0044	83.9562	106.7924	89.7095	100.062	93.1325
A(81,83,92) ≡ A(81,83,87)	-	-	133.926	126.358	110.486	113.275	117.838	107.354

≡ A(80,82,87)			3	9	3	6	3	
A(25,92,41) ≡ A(25,87,41)	-	-	38.0046	53.8461	43.304	47.9201	82.1022	85.6303
A(25,92,67)≡A(25,87,67) ≡A(25,87,66)	-	-	120.7211	119.2639	147.1056	147.5593	112.4471	109.7756
A(25,92,83) ≡ A(25,87,83) ≡A(25,87,82)	-		108.0868	121.3292	152.1263	143.9749	163.0407	165.3994
A(25,92,84) ≡ A(25,87,84)	-	-	84.4529	136.2762	103.7502	119.6505	-	-
A(25,92,85) ≡ A(25,87,85)	-	-	83.1682	111.3137	98.578	76.1812	-	-
A(41,92,67)≡A(41,87,67) ≡A(41,87,66)	-	-	151.7132	141.8668	168.1202	164.2734	163.3235	164.2685
A(41,92,83) ≡A(41,87,83) ≡A(41,87,82)	-	-	146.0914	174.7884	120.976	123.5	84.7979	80.1362
A(41,92,84) ≡ A(41,87,84)	-	-	49.4506	83.6243	67.0675	78.2885	-	-
A(41,92,85) ≡ A(41,87,85)	-	-	73.2754	101.1953	106.0995	110.3395	-	-
A(67,92,83) ≡ A(67,87,83) ≡ (66,87,82)	-	-	51.0673	41.0377	47.1878	48.2682	82.2504	84.2874
A(67,92,84) ≡ A(67,87,84)	-	-	130.1122	86.6976	106.6149	87.0066	-	-
A(67,92,85) ≡ A(67,87,85)	-	-	130.7652	114.0228	70.0202	82.181	-	-
A(83,92,84) ≡ A(83,87,84)	-	-	164.7116	101.5365	81.8855	84.0045	-	-
A(83,92,85) ≡ A(83,87,85)	-	-	81.7917	78.1593	60.2731	77.216	-	-
A(84,92,85) ≡ A(84,87,85)	-	-	91.3371	82.6781	131.6509	161.0912	-	-
Dihedral Angles (degree)								
D(20,21,25,92) ≡D(20,21,25,87)		-	-	9.9413	8.6197	13.5972	32.1584	91.5666	71.9974
D(29,21,25,92) ≡ D(29,21,25,87)	-	-	-113.313	-107.049	-110.157	-85.0	-48.2794	-63.5871
D(20,22,25,92) ≡ D(20,22,25,87)	-	-	-174.455	175.9174	-155.325	-144.977	-108.859	-115.032
D(26,22,25,92) ≡ D(26,22,25,87)	-	-	0.9959	-6.349	25.7466	43.1049	72.7298	74.8193
D(92,25,27,28) ≡ D(87,25,27,28)	-	-	-134.343	-127.67	-140.062	-144.337	-160.583	-147.029
D(92,25,27,30) ≡ D(87,25,27,30)	-	-	109.4272	116.2357	104.9851	99.4079	82.979	93.682
D(92,25,27,39) ≡ D(87,25,27,39)	-	-	-19.2259	-12.5396	-21.7074	-29.1777	-40.4559	-30.4182
D(21,25,92,41) ≡ D(21,25,87,41)	-	-	-170.299	164.1065	147.3435	154.8796	151.9994	167.8784
D(21,25,92,67) ≡ D(21,25,87,67) ≡D(21,25,87,66)	-	-	-15.7249	-60.881	-23.2961	-29.4961	-36.4734	-8.8542
D(21,25,92,83) ≡ D(21,25,87,83) ≡D(21,25,87,82)	-	-	39.1819	-13.0347	80.9904	63.5756	112.2378	155.0135
D(21,25,92,84) ≡ D(21,25,87,84)	-	-	-149.774	179.7558	179.7247	-171.084	-	-

D(21,25,92,85) ≡ D(21,25,87,85)	≡	-	-	118.206	76.4249	42.9346	20.1015	-	-
D(22,25,92,41) ≡ D(22,25,87,41)	≡	-	-	-158.845	167.3988	175.4859	-157.341	107.381	101.132
D(22,25,92,67) ≡ D(22,25,87,67) ≡D(22,25,87,66)	≡	-	-	-4.2708	-57.5886	4.8462	18.2835	64.146	82.1356
D(22,25,92,83) ≡ D(22,25,87,83) ≡D(22,25,87,82)	≡	-	-	50.6359	-9.7423	109.1327	111.3552	-147.143	-113.997
D(22,25,92,84) ≡ D(22,25,87,84)	≡	-	-	-138.32	-176.952	-152.133	-123.305		
D(22,25,92,85) ≡D(22,25,87,85)		-	-	129.66	79.7173	71.0769	67.881	-	-
D(27,25,92,41) ≡ D(27,25,87,41)	≡	-	-	45.8801	26.995	3.1986	32.5202	35.9668	42.3072
D(27,25,92,67) ≡ D(27,25,87,67) ≡D(27,25,87,66)	≡	-	-	-159.545	162.0076	-167.441	-151.856	-152.506	-134.425
D(27,25,92,83) ≡ D(27,25,87,83) ≡D(27,25,87,82)	≡	-	-	-104.639	-150.146	-63.1545	-58.7838	-3.7948	29.4424
D(27,25,92,84) ≡ D(27,25,87,84)	≡	-	-	66.4054	42.6444	35.5798	66.5563	-	-
D(27,25,92,85) ≡D(27,25,87,85)		-	-	-25.6145	-60.6866	-101.210	-102.258	-	-
D(27,39,41,92) ≡ D(27,39,41,87)	≡	-	-	116.5855	65.3777	-55.5422	51.1453	8.4834	36.9815
D(40,39,41,92) ≡ D(40,39,41,87)	≡	-	-	-61.1852	-120.055	125.7427	-131.783	-170.984	-148.468
D(39,41,92,25) ≡ D(39,41,87,25)	≡	-	-	-60.5104	-50.8076	32.4142	-49.5154	-26.8391	-47.0943
D(39,41,92,67) ≡D(39,41,87,67) ≡D(39,41,87,66)		-	-	-111.666	-143.657	-172.995	139.1691	-178.510	121.4959
D(39,41,92,84) ≡ D(39,41,87,84)	≡	-	-	146.83	140.0055	-113.194	160.2709	-	-
D(39,41,92,85) ≡ D(39,41,87,85)	≡	-	-	40.0229	58.7971	117.8317	-2.1972	-	-
D(42,41,92,25) ≡ D(42,41,87,25)	≡	-	-	165.3824	173.7012	154.2401	169.2781	-	-
D(42,41,92,67) ≡ D(42,41,87,67)	≡	-	-	114.2271	80.8516	-51.1692	-2.0374	-	-
D(42,41,92,84) ≡ D(42,41,87,84)	≡	-	-	12.7229	4.5144	8.6316	19.0645	-	-
D(42,41,92,85) ≡ D(42,41,87,85)	≡	-	-	-94.0842	-76.6941	-120.343	-143.404	-	-
D(62,63,67,92) ≡ D(62,63,67,87) ≡D(61,62,66,87)	≡	-	-	15.9032	19.1231	-16.2532	12.4606	-101.979	139.0518
D(71,63,67,92) ≡ D(71,63,67,87) ≡D(70,62,66,87)	≡	-	-	-105.636	-97.7313	-138.313	-102.295	140.7008	133.062
D(62,64,67,92) ≡	≡	-	-	-	-	162.772	176.183	129.602	-

D(62,64,67,87) ≡D(61,63,66,87)				174.678	170.886	8	2	3	114.609
D(68,64,67,92) ≡ D(68,64,67,87) ≡D(67,63,66,87)	≡	-	-	3.5197	11.1512	-16.7731	-1.9198	-48.1237	-40.9958
D(92,67,69,72) ≡ D(87,67,69,72) ≡D(87,66,68,71)	≡	-	-	111.7738	114.5758	123.7352	112.6399	177.3121	-179.993
D(92,67,69,81) ≡ D(87,67,69,81) ≡D(87,66,68,80)	≡	-	-	-17.1679	-11.7318	-6.2678	-14.761	46.1278	52.3627
D(63,67,92,25) ≡ D(63,67,87,25) ≡D(62,66,87,25)	≡	-	-	-92.9628	-87.7617	-23.855	-57.318	0.4814	-4.2502
D(63,67,92,41) ≡D(63,67,87,41) ≡D(62,66,87,41)		-	-	-59.0561	-20.1817	-171.043	110.6229	149.9132	-172.151
D(63,67,92,83) ≡ D(63,67,87,83) ≡D(62,66,87,82)	≡	-	-	177.9429	166.9277	-165.714	174.5855	-170.724	179.7863
D(63,67,92,84) ≡ D(63,67,87,84)	≡	-	-	17.7448	55.1254	132.7912	89.9512	-	-
D(63,67,92,85) ≡ D(63,67,87,85)	≡	-	-	157.7916	135.6003	-98.1974	-105.598	-	-
D(64,67,92,25) ≡ D(64,67,87,25) ≡D(63,66,87,25)	≡	-	-	-77.0551	-67.1301	-48.2871	-51.0662	-100.758	-115.607
D(64,67,92,41) ≡ D(64,67,87,41) ≡D(63,66,87,41)	≡	-	-	-43.1484	0.4498	164.525	116.8748	48.6737	76.4924
D(64,67,92,83) ≡ D(64,67,87,83) ≡D(63,66,87,82)	≡	-	-	-166.149	-172.441	169.8543	-179.163	88.0362	68.4293
D(64,67,92,84) ≡ D(64,67,87,84)	≡	-	-	33.6525	75.7569	108.359	96.2031	-	-
D(64,67,92,85) ≡ D(64,67,87,85)	≡	-	-	173.6993	156.2319	-122.63	-99.3464	-	-
D(69,67,92,25) ≡ D(69,67,87,25) ≡D(68,66,87,25)	≡	-	-	123.3534	147.1481	167.4743	169.9367	133.0401	122.8208
D(69,67,92,41) ≡ D(69,67,87,41) ≡D(68,66,87,41)	≡	-	-	157.26	-145.272	20.2864	-22.1223	-77.5281	-45.0796
D(69,67,92,83) ≡ D(69,67,87,83) ≡D(68,66,87,82)	≡	-	-	34.2591	41.8375	25.6157	41.8403	-38.1656	-53.1427
D(69,67,92,84) ≡ D(69,67,87,84)	≡	-	-	-125.939	-69.9648	-35.8796	-42.794	-	-
D(69,67,92,85) ≡ D(69,67,87,85)	≡	-	-	14.1077	10.5102	93.1318	121.6564	-	-
D(69,81,83,92) ≡ D(69,81,83,87) ≡D(68,80,82,87)	≡	-	-	77.2108	110.9268	78.0503	95.441	-1.0654	-18.264
D(82,81,83,92) ≡	≡	-	-	-	-	-	-88.530	175.807	162.819

D(82,81,83,87) ≡D(81,80,82,87)			107.801	74.0742	109.639		6	1
D(81,83,92,25) ≡ (81,83,87,25) ≡D(80,82,87,25)			-176.924	-178.73	178.0222	163.7235	-127.127	-120.98
D(81,83,92,67) ≡ D(81,83,87,67) ≡D(80,82,87,66)	-	-	-61.6453	-78.804	-47.8205	-62.1479	23.898	43.7848
D(81,83,92,84) ≡ D(81,83,87,84)	-	-	39.0648	-7.7118	73.9021	29.1882	-	-
D(81,83,92,85) ≡ D(81,83,87,85)	-	-	103.0696	72.1692	-137.398	-153.033	-	-

-Numerations of atoms were done according to optimized structures in (Figures 14 -17).

The results show good agreement with the structures suggested from the analytical data.

Frontier Molecular Orbitals analysis (HOMO-LUMO analyses):

Knowledge of the HOMO and LUMO, and their properties namely their energy, is very useful to gauge the chemical reactivity of molecules. During molecular interactions, the LUMO accepts electrons and its energy corresponds to the electron affinity (EA), while the HOMO represents electron donors and its energy is associated with the ionization potential (IP) [39]. Smaller is the HUMO-LUMO gap (HLG) softer is the complex [40, 41].

Amoxicillin ligand

The highest occupied molecular orbital (HOMO) is mainly localized on the carbon atoms of the ring of Amoxicillin, while the lowest unoccupied molecular orbital (LUMO) is mainly localized on the carboxylic group. The energy gap between the HOMO and LUMO energies has been calculated as 5.52 eV (Fig. 18). This large energy gap characterizes a high chemical hardness and kinetic stability of the coordination compound [42]. As a consequence, this compound is stable in standard conditions.
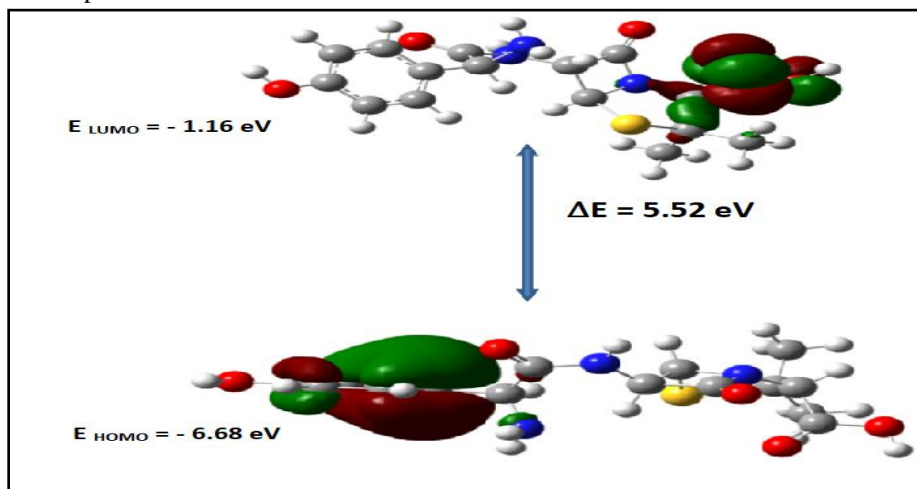

Figure 18: HOMO and LUMO structures of Amoxicillin ligand

Amoxicillin- Cupper complex

The highest occupied molecular orbital (HOMO) is mainly localized on the carbon atoms of one ring of Amoxicillin, while the lowest unoccupied molecular orbital (LUMO) is mainly localized on one of the 5-membered thiazolidine rings. The energy gap between the HOMO and LUMO energies had been calculated as 4.2 eV (Fig. 19).
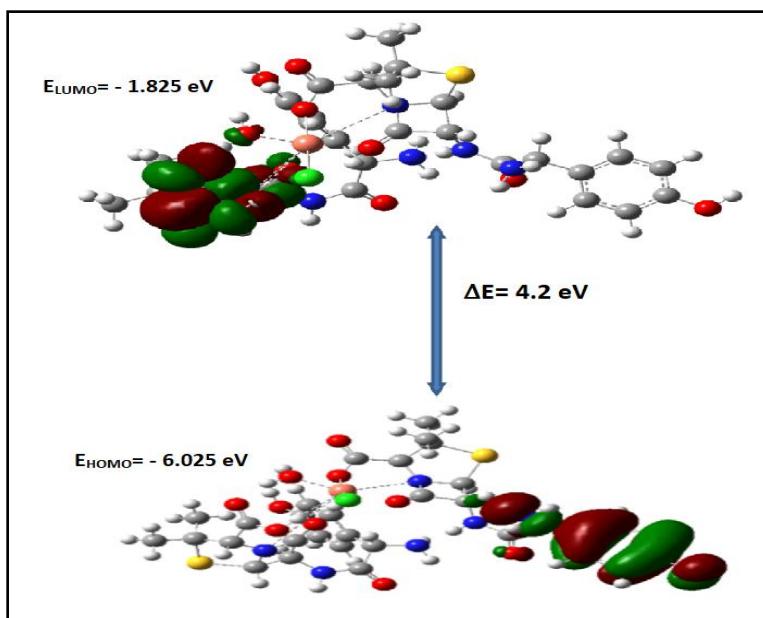
Figure 19: HOMO and LUMO structures of Amoxicillin-Cu complex

Amoxicillin- Zinc complex

The highest occupied molecular orbital (HOMO) is mainly localized on the carbon atoms of one ring of Amoxicillin, while the lowest unoccupied molecular orbital (LUMO) is mainly localized on one of the 5-membered thiazolidine rings. The energy gap between the HOMO and LUMO energies had been calculated as 3.55 eV (Fig.20).
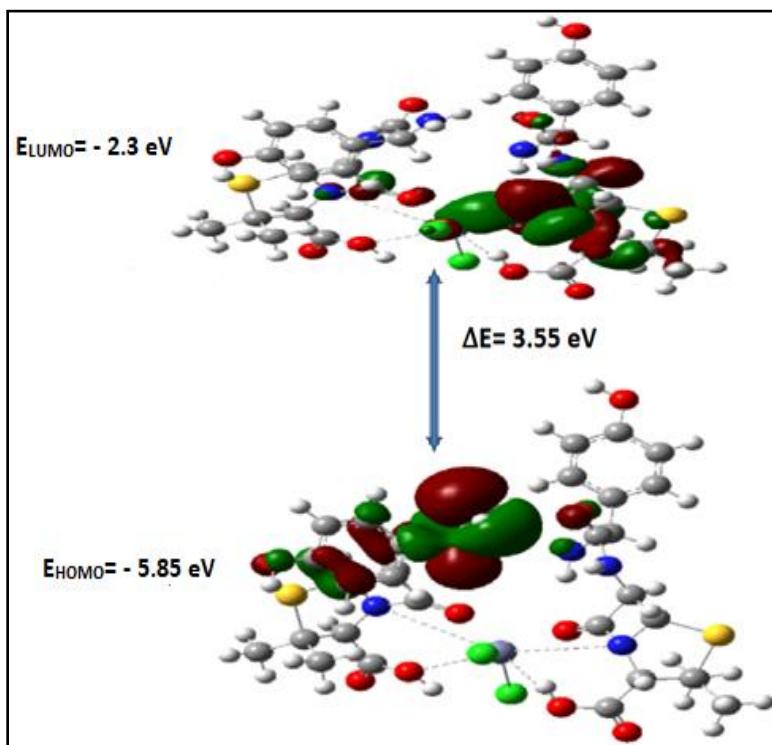

Figure 20: HOMO and LUMO structures of Amoxicillin-Zn complex Amoxicillin- Nickel complex

The highest occupied molecular orbital (HOMO) is mainly localized on the carbon atoms and hydroxyl group of one ring of Amoxicillin, and also on the Nitrogen atom next to the ring while the lowest unoccupied molecular orbital (LUMO) is mainly localized on the metal atom and all the surrounding Oxygen and Nitrogen atoms. The energy gap between the HOMO and LUMO energies had been calculated as 2.91 eV (Fig.21).
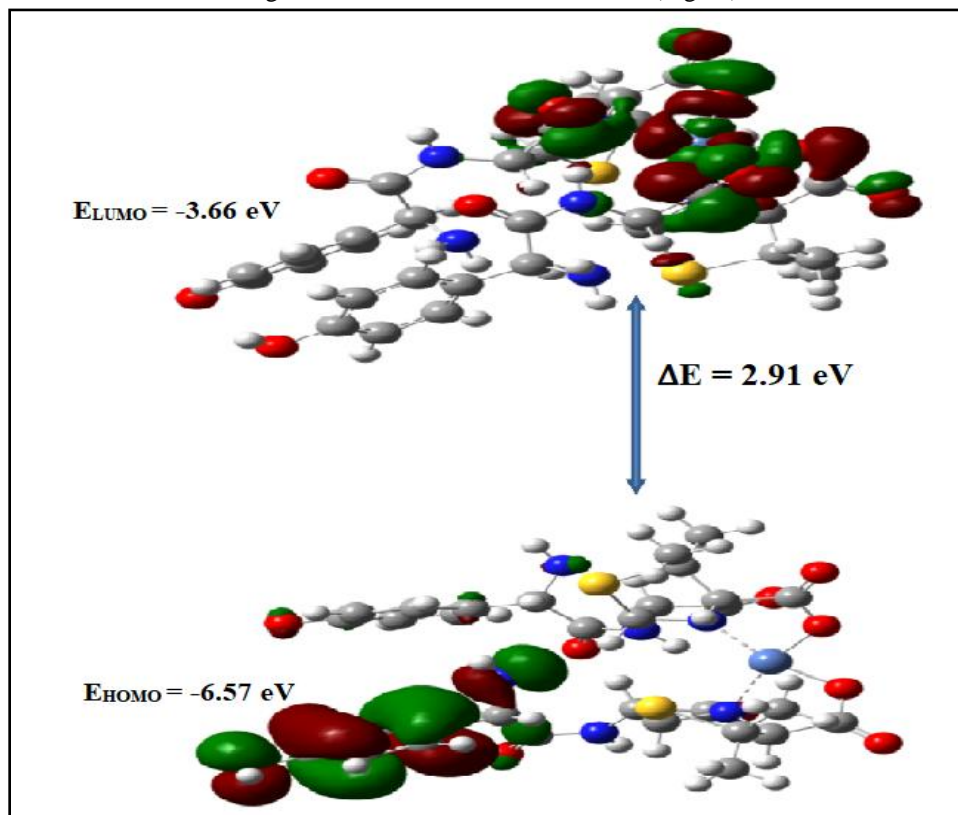

Figure 21: HOMO and LUMO structures of Amoxicillin-Ni complex

It is predicted from the HOMO-LUMO gaps that the title complexes are soft as is obvious from their smaller HUMO-LUMO energy gaps (HLG) [43-44].

The HOMO-LUMO energy gap explains the concluding charge transfer interaction within the molecule and is useful in determining molecular electrical transport properties. A molecule with a high frontier orbital gap (HOMO-LUMO energy gap) has low chemical reactivity and high kinetic stability, because it is energetically unfavorable to add an electron to the high-lying LUMO in order to remove electrons from the low-lying HOMO. For instance, compounds that have a high HOMO-LUMO energy gap are stable, and hence are chemically harder than compounds having a small HOMO-LUMO energy gap [45].

Thus, it is clear from Table (8) that Amoxicillin is hard and more stable (less reactive), while Amoxicillin Nickel complex is soft and the least stable of all (more reactive) in the studied complexes as The HOMO-LUMO energy gap decreases from Amoxicillin to Amoxicillin Nickel complex.

Table 8: The computed HOMO and LUMO energies and Energy gaps for Amoxicillin and its metal complexes:

	E_{LUMO} (eV)	E_{HOMO} (eV)	Energy gap (ΔE) (eV)	Dipole moment (μ) (D)
Amoxicillin	-1.16	-6.6	5.52	-
Cu complex	-1.825	-6.025	4.2	5.5375
Zn complex	-2.3	-5.85	3.55	2.1484
Ni complex	-3.66	-6.57	2.91	13.0821

Charge transfer

The Mulliken population analysis [46, 47] is probably the best known of all models for predicting individual atomic charges which is computationally very popular due to its simplicity. Mulliken charges were shown to be highly basis set dependent and unpredictable with marked fluctuations in partial charges [48]. The obtained results are illustrated in detail in Table 9.

In All prepared Amoxicillin complexes, all the atoms attached to metal atom are found to be negatively charged, while metal atoms is found to be positively charged, which may be due to the attachment of metal atom to highly electronegative atoms. As can be seen in Table 9, in Cu complex, the Oxygen atom (of coordinated water) has the most negative charge. In Zn complex, the chlorine atom coordinated to the metal ion has the most negative charge but in Ni complex, the N atom coordinated to the metal ion has the most negative charge. The result suggests that the metal atoms are electron acceptors and also indicates the charge transfer from all coordinated atoms (N, O, Cl) to them. These calculations showed the electronegative nature of the O, N, and Cl atoms.

The decrease in the HOMO-LUMO energy gap explains the eventual charge transfer interaction taking place within the studied compounds because of the strong electron-accepting ability of the electron acceptor atoms. So, According to the calculated atomic charge, there is a charge transfer from the ligand to the metal ion.

For Amoxicillin Cupper complex, the charge of Cu before complexation was +2 and after complexation it became (0.479 – 0.954) by using DFT and PM6 calculations, respectively. The charge transfer from Amoxicillin ligand to Cu metal atom was (1.521- 1.046). For Amoxicillin Zinc complex, the charge of Zn before complexation was +2 and after complexation it became (0.719 – 0.372) by using DFT and PM6 calculations, respectively. The charge transfer from Amoxicillin ligand to Zn metal atom was (1.281- 1.628) while for For Amoxicillin Nickel complex, the charge of Ni before complexation was +2 and after complexation it became (0.378 – 0.788) by using DFT and PM6 calculations, respectively. The charge transfer from Amoxicillin ligand to Ni metal atom was (1.622- 1.212). So, the charge transfer from ligand to metal ion follows the trend Amoxicillin Nickel > Amoxicillin Cupper > Amoxicillin Zinc complex by using DFT calculations, but by using PM6 calculations, the trend became Amoxicillin Zinc > Amoxicillin Nickel >Amoxicillin Cupper complex.

Table 9: Mulliken atomic charges of Amoxicillin and its metal complexes calculated by MP6 and DFTB3LYP /LANL2DZ methods, L1= first coordinated molecule of amoxicillin, L2= second coordinated molecule of amoxicillin

Atom	Amoxicillin		Cu complex		Zn complex		Ni complex	
	DFT	PM6	DFT	PM6	DFT	PM6	DFT	PM6
L1 N	-0.142780	-0.440657	-0.112037	-0.377241	-0.133629	-0.416149	-0.330927	-0.365641
L1 O	-0.450189	-0.523242	-0.405062	-0.480667	-0.473251	-0.477862	-0.317515	-0.465913
L2 N	-0.142780	-0.440657	-0.108950	-0.477771	-0.116664	-0.415586	-0.357118	-0.475825
L2 O	-0.450189	-0.523242	-0.506538	-0.631595	-0.419442	-0.479040	-0.315979	-0.437370
Cl1 atom	-	-	-0.352060	-0.483497	-0.488687	-0.462019	-	-
Cl2 atom	-	-	-	-	-0.431066	-0.391762	-	-
O of H_2O	-	-	-0.727424	-0.636684	-	-	-	-
Metal atom	-	-	0.479599	0.953871	0.718989	0.371883	0.377627	0.788141

Experimental and Theoritical UV values

From the optained data, there is Agood agreement between Experimental and Theoritical UV values for Amoxicillin and its metal complexes (Table 10) which enhance the supposed structures.

Table 10: Experimental and Theoritical values of UV

	Theoritical excitation energy		Experimental excitation energy (UV)
Amoxicillin	1st excitaion state	277.15 nm	385
	2nd excitaion state	271.56 nm	290
	3rd excitaion state	257.64 nm	
Cu complex	1st excitaion state	894.40 nm	430
	2nd excitaion state	812.88 nm	355
	3rd excitaion state	764.99 nm	325
Zn complex	1st excitaion state	402.80 nm	410
	2nd excitaion state	368.26 nm	355
	3rd excitaion state	362.59 nm	325

Conclusion

Characterization of the new complexes of Mn (II), Fe (III), Ni (II), Cu (II), Zn(II) and Cd (II) with Amoxicillin was investigated. The result of this investigation supported the suggested structure of the metal complexes. Based on the data obtained. The ligand coordinated to the metal ions through $v(N)$ and $v(COO)$ due to their structural similarities. The elemental percentages are also in good agreement with the proposed structure. Only Nickel complex has one water molecule outside its coordination sphere. An octahedral structure was suggested for all complexes except Nickel complex which showed a tetrahedral structure. Molecular modelling of the ligands was done and all Molecular modelling data were calculated.

Thermal analysis of the metal complexes of Amoxicillin proved that these complexes are more thermally stable than Amoxicillin. The ligand was found to be biologically active and its metal complexes display enhanced antimicrobial activity against some strains, chelation tends to make the ligands act as more powerful and potent bactericidal agent. So, Complexation improves the Thermal stability and biological activity of the investigated ligands. Optimization of the supposed structures of complexes was done to obtain the lowest energy structure and the optimized parameters were calculated which show good agreement with the experimental data.

Reference

[1]. J. Adediji, E. Olayinka, M. Adebayo, O. Babatunde, Antimalarial mixed ligand metal complexes: synthesis, physicochemical and biological activities, International Journal of Physical Sciences, 4 (2009) 529-534.

[2]. T. Wang, Z. Guo, Copper in medicine: homeostasis, chelation therapy and antitumor drug design, Current medicinal chemistry, 13 (2006) 525-537.

[3]. I.M. Kenawi, B.N. Barsoum, M.A. Youssef, Drug–drug interaction between diclofenac, cetirizine and ranitidine, Journal of pharmaceutical and biomedical analysis, 37 (2005) 655-661.

[4]. J.J. Nogueira Silva, W.R. Pavanelli, F.R. Salazar Gutierrez, F.C. Alves Lima, A.B. Ferreira da Silva, J.o. Santana Silva, D. Wagner Franco, Complexation of the anti-Trypanosoma cruzi drug benznidazole improves solubility and efficacy, Journal of Medicinal Chemistry, 51 (2008) 4104-4114.

[5]. V.A. Marcolino, G.M. Zanin, L.R. Durrant, M.D.T. Benassi, G. Matioli, Interaction of curcumin and bixin with β-cyclodextrin: complexation methods, stability, and applications in food, Journal of agricultural and food chemistry, 59 (2011) 3348-3357.

[6]. S. Lapshin, V. Alekseev, Copper (II) complexation with ampicillin, amoxicillin, and cephalexin, Russian Journal of Inorganic chemistry, 54 (2009) 1066-1069.

[7]. M.S. Iqbal, I.H. Bukhari, M. Arif, Preparation, characterization and biological evaluation of copper (II) and zinc (II) complexes with Schiff bases derived from amoxicillin and cephalexin, Applied organometallic chemistry, 19 (2005) 864-869.

[8]. M. Zayed, S. Abdallah, Synthesis and structure investigation of the antibiotic amoxicillin complexes of d-block elements, Spectrochimica Acta Part A: Molecular and Biomolecular Spectroscopy, 61 (2005) 2231-2238.

[9]. M. Imran, J. Iqbal, T. Mehmood, S. Latif, Synthesis, characterization and in vitro screening of amoxicillin and its complexes with Ag (I), Cu (II), Co (II), Zn (II) and Ni (II), J. Biol. Sci, 6 (2006) 946-949.

[10]. M. Kurt, T. Sertbakan, M. Özduran, An experimental and theoretical study of molecular structure and vibrational spectra of 3-and 4-pyridineboronic acid molecules by density functional theory calculations, Spectrochimica Acta Part A: Molecular and Biomolecular Spectroscopy, 70 (2008) 664-673.

[11]. J. Adekoya, Synthesis, characterization, antimicrobial activity and toxicology study of some metal complexes of mixed antibics, A frican J ournalof P ureand A pplied C hemistry, 2 (2008) 069-074.

[12]. K. Ogunniran, A. Tella, M. Alensela, M. Yakubu, Synthesis, physical properties, antimicrobial potentials of some antibiotics complexed with transition metals and their effects on alkaline phosphatase activities of selected rat tissues, African Journal of Biotechnology, 6 (2007) 1202.

[13]. C. Bayrak, N. Secken, F.O. Ozturk, E.U. ALSAN, A simulation on teaching volhard method, Turkish Online Journal of Distance Education, 10 (2009) 105-116.

[14]. K. Nakamoto, Infrared and Raman spectra of inorganic and coordination compounds, part B: applications in coordination, organometallic, and bioinorganic chemistry, John Wiley & Sons2009.

[15]. T.H. Al-Noor, A.J. Jarad, A.O. Hussein, Synthesis, Physico-Chemical and Antimicrobial Properties of Some Metal (II)-Mixed Ligand Complexes of Tridentate Schiff Base Derives From B-Lactam antibiotic {(cephalexin mono hydrate)-4-chlorobenzophenone} and saccharin, International Journal of Chemical and Process Engineering Research, 1 (2014) 109-120.

[16]. A.L. Demain, R.P. Elander, The β-lactam antibiotics: past, present, and future, Antonie Van Leeuwenhoek, 75 (1999) 5-19.

[17]. E.L. Miller, The penicillins: a review and update, Journal of midwifery & women's health, 47 (2002) 426-434.

[18]. A. Chakravorty, Structural chemistry of transition metal complexes of oximes, Coordination Chemistry Reviews, 13 (1974) 1-46.

[19]. M.S. Masoud, A.E. Ali, G.S. Elasala, S.A. Kolkaila, Synthesis, spectroscopic, biological activity and thermal characterization of ceftazidime with transition metals, Spectrochimica Acta Part A: Molecular and Biomolecular Spectroscopy, 193 (2018) 458-466.

[20]. E.K. Barefield, D. Busch, S. Nelson, Iron, cobalt, and nickel complexes having anomalous magnetic moments, Quarterly Reviews, Chemical Society, 22 (1968) 457-498.

[21]. A. Sreekanth, M. Joseph, H.-K. Fun, M.P. Kurup, Formation of manganese (II) complexes of substituted thiosemicarbazones derived from 2-benzoylpyridine: Structural and spectroscopic studies, Polyhedron, 25 (2006) 1408-1414.

[22]. R. Atkins, G. Brewer, E. Kokot, G.M. Mockler, E. Sinn, Copper (II) and nickel (II) complexes of unsymmetrical tetradentate Schiff base ligands, Inorganic Chemistry, 24 (1985) 127-134.

[23]. P. Guru, Studies of two Complexes with Ampicillin, Int. J. of Chem. Tech. Research, 1 (2009) 461-463.

[24]. M.S. Masoud, A.E. Ali, G.S. Elasala, S.F. Sakr, S.A. Kolkaila, Physicochemical Studies of Some Biologically Active Metal Complexes of Cefazolin Antibiotics, Journal of Chemical and Pharmaceutical Research, 12 (2020) 42-52.

[25]. M. Masoud, E. Khalil, A. Hafez, A. El-Husseiny, Electron spin resonance and magnetic studies on some copper (II) azobarbituric and azothiobarbituric acid complexes, Spectrochimica Acta Part A: Molecular and Biomolecular Spectroscopy, 61 (2005) 989-993.

[26]. M.S. Masoud, S.S. Hagagg, A.E. Ali, N.M. Nasr, Synthesis and spectroscopic characterization of gallic acid and some of its azo complexes, Journal of Molecular Structure, 1014 (2012) 17-25.

[27]. B. Behera, J. Behera, Drug metal ion interaction: kinetics and mechanism of interaction of cis-bis (oxalate) diaquochromium (III) ion with ampicillin in aqueous medium, Chem Sci Trans, 6 (2017) 535-544.

[28]. R. Di Stefano, M. Scopelliti, C. Pellerito, T. Fiore, R. Vitturi, M. Colomba, P. Gianguzza, G. Stocco, M. Consiglio, L. Pellerito, Organometallic complexes with biological molecules: XVII. Triorganotin (IV) complexes with amoxicillin and ampicillin, Journal of inorganic biochemistry, 89 (2002) 279-292.

[29]. P. Mishra, Biocoordination, Computational Modeling and Antibacterial Sensitivities of Cobalt (II), Nickel (II), Copper (II) and Bismuth (V) with Gentamicin and Amoxicillin Antibiotics mixed Ligands, International Journal of Pharmaceutical Sciences Review and Research, 3 (2010) 145-156.

[30]. F.I. Eze, U. Ajali, P.O. Ukoha, Synthesis, physicochemical properties, and antimicrobial studies of Iron (III) complexes of ciprofloxacin, cloxacillin, and amoxicillin, International journal of medicinal chemistry, 2014 (2014).

[31]. M.S. Masoud, A.E. Ali, G.S. Elasala, S. Kolkaila, Spectroscopic studies and thermal analysis on cefoperazone metal complexes, J. Chem. Pharm. Res, 9 (2017) 171-179.

[32]. M.S. Masoud, A.E. Ali, G.S. Elasala, Synthesis, spectral, computational and thermal analysis studies of metallocefotaxime antibiotics, Spectrochimica Acta Part A: Molecular and Biomolecular Spectroscopy, 149 (2015) 363-377.

[33]. M.S. Masoud, A.E. Ali, M.Y. Abd El-Kaway, Thermal properties of mercury (II) and palladium (II) purine and pyrimidine complexes, Journal of Thermal Analysis and Calorimetry, 116 (2014) 183-194.

[34]. A.E. Ali, G.S. Elasala, E.A. Mohamed, S.A. Kolkaila, Spectral, thermal studies and biological activity of pyrazinamide complexes, Heliyon, 5 (2019) e02912.

[35]. G. Piloyan, I. Ryabchikov, O. Novikova, Determination of activation energies of chemical reactions by differential thermal analysis, Nature, 212 (1966) 1229-1229.

[36]. H.E. Kissinger, Reaction kinetics in differential thermal analysis, Analytical chemistry, 29 (1957) 1702-1706.

[37]. R. Kumar, S. Obrai, Quantum Computational Chemistry: Modeling and Calculation of S-Block Metal Ion Complexes, Density Functional Theory Calculations, IntechOpen2020.

[38]. S.M. Soliman, A. Barakat, M.S. Islam, H.A. Ghabbour, Synthesis, crystal structure and DFT studies of a new dinuclear Ag (I)-malonamide complex, Molecules, 23 (2018) 888.

[39]. K. Fukui, T. Yonezawa, H. Shingu, A molecular orbital theory of reactivity in aromatic hydrocarbons, The Journal of Chemical Physics, 20 (1952) 722-725.

[40]. G. Mariappan, N. Sundaraganesan, Spectral and structural studies of the anti-cancer drug Flutamide by density functional theoretical method, Spectrochimica Acta Part A: Molecular and Biomolecular Spectroscopy, 117 (2014) 604-613.

[41]. I. Fleming, Frontier orbitals and organic chemical reactions, Wiley1977.

[42]. X.H. Li, X.R. Liu, X.Z. Zhang, Molecular structure and vibrational spectra of three substituted 4-thioflavones by density functional theory and ab initio Hartree–Fock calculations, Spectrochimica Acta Part A: Molecular and Biomolecular Spectroscopy, 78 (2011) 528-536.

[43]. V. Balachandran, S. Lalitha, S. Rajeswari, V. Rastogi, Theoretical investigations on the molecular structure, vibrational spectra, thermodynamics, HOMO–LUMO, NBO analyses and paramagnetic susceptibility properties of p-(p-hydroxyphenoxy) benzoic acid, Spectrochimica Acta Part A: Molecular and Biomolecular Spectroscopy, 121 (2014) 575-585.

[44]. Y. Uesugi, M. Mizuno, A. Shimojima, H. Takahashi, Transient resonance Raman and ab initio MO calculation studies of the structures and vibrational assignments of the T1 state and the anion radical of coumarin and its isotopically substituted analogues, The Journal of Physical Chemistry A, 101 (1997) 268-274.

[45]. Y. Ruiz-Morales, HOMO− LUMO gap as an index of molecular size and structure for polycyclic aromatic hydrocarbons (PAHs) and asphaltenes: A theoretical study. I, The Journal of Physical Chemistry A, 106 (2002) 11283-11308.

[46]. R. Mulliken, Electronic population analysis on LCAO–MO molecular wave functions. II. Overlap populations, bond orders, and covalent bond energies, The Journal of Chemical Physics, 23 (1955) 1841-1846.

[47]. R. Mulliken, Criteria for the construction of good self-consistent-field molecular orbital wave functions, and the significance of lCAO-MO population analysis, The Journal of Chemical Physics, 36 (1962) 3428-3439.

[48]. J. Rigby, E.I. Izgorodina, Assessment of atomic partial charge schemes for polarisation and charge transfer effects in ionic liquids, Physical Chemistry Chemical Physics, 15 (2013) 1632-1646.